Electronic Supplementary Information (ESI)

Urea-engineering mediated hydrogen-bond donating Friedel–Crafts alkylation of indoles and nitroalkenes in dual-functionalized microporous metal-organic framework with high recyclability and pore-fitting-induced size-selectivity

Manpreet Singh,[ab] and Subhadip Neogi *[ab]

[a]Inorganic Materials & Catalysis Division, CSIR-Central Salt and Marine Chemicals Research Institute (CSIR-CSMCRI), Bhavnagar, Gujarat 364002, India
[b]Academy of Scientific and Innovative Research (AcSIR), Ghaziabad- 201002, India
*E-mail (SN): sneogi@csmcri.res.in

Materials and physical measurements

All the solvents and reagents were purchased from commercial sources (except H_3TCA) and used without further purification. TCA and Ligand L were synthesised as per experimental section. Powder X-ray diffraction (PXRD) data were collected using a PANalytical Empyrean (PIXcel 3D detector) system equipped with Cu K_α (λ=1.54 Å) radiation. The Fourier Transform Infrared-spectra (FT-IR) of the samples were recorded using the KBr pellet method on a Perkin–Elmer GX FTIR spectrometer in the region of 4000−400 cm^{-1}. Surface area and gas sorption measurement was carried out using Quantachrome Autosorb IQ instrument. Thermogravimetric analyses (TGA) (heating rate of 5 °C/min under N_2 atmosphere) were performed with a Mettler Toledo Star SW 8.10 system. ^1H and ^{13}C NMR spectra were recorded on a Bruker Avance-II 500 MHz NMR spectrometer. Scanning Electron Microscopic (SEM) and Transmission Electron Microscopic (TEM) images were obtained with a JEOL JSM 7100F and JEOL, JEM 2100 instrument, respectively. XPS analysis was carried out using a Thermo Scientific ESCALAB 250 Xi photoelectron spectrometer (XPS) using a monochromatic Al Kα X-ray as an excitation source. Inductively coupled plasma-optical emission spectrometry (ICP-OES) analysis was measured by Perkin Elmer, Optima 2000 Microanalyses of the compounds were conducted using elementarvario MICRO CUBE analyser. Molecular dimensions of the molecule were calculated from the freely available software Avogadro.[1]

Single crystal X-ray crystallography

Single crystals with suitable dimensions were chosen under an optical microscope and mounted on a glass fibre for data collection. The crystal data for as synthesized block shaped crystal of **CSMCRI-12** were collected on a Bruker D8 Quest diffractometer, with CMOS detector in shutter less mode. The crystals were cooled to low temperature using an Oxford Cryostream liquid nitrogen cryostat. The instrument was equipped with a graphite monochromatized MoKα X-ray source (λ = 0.71073 Å), with Triumph™ X-ray source optics. Data collection and initial indexing and cell refinement were handled using APEX II software.[2] Frame integration, including Lorentz-polarization corrections, and final cell parameter calculations were carried out using SAINT+ software.[3] The data were corrected for absorption using the SADABS program.[4] Decay of reflection intensity was monitored by analysis of redundant frames. The structure was solved using Direct methods and difference Fourier techniques. All non-hydrogen atoms were refined anisotropically. All H atoms were placed in calculated positions using idealized geometries (riding model) and assigned fixed isotropic displacement parameters. The SHELXL-2014 package within the OLEX2 crystallographic software[5] was applied for structure refinement with several full-matrix least-squares/difference Fourier cycles.[6] The disordered guest solvent molecules in the crystal lattice were treated with solvent mask option in OLEX2 software.[5] The potential solvent accessible void space was calculated using the PLATON[7] software. The crystal and refinement data for solvent free **CSMCRI-12** is listed in Table S1. Topological analysis was performed by using TOPOSPro software.[8]

Synthesis of ligands:

4,4′,4″-tricarboxytriphenylamine (H_3TCA)

Ligand was synthesized and characterised following similar protocol, reported from our group.[9]

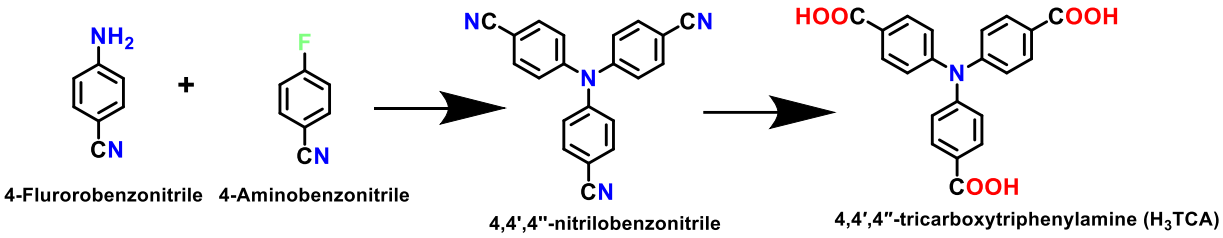

Scheme 1. Synthesis of ligand (H_3TCA).

1,3-di(pyridin-4-yl)urea (*L*)

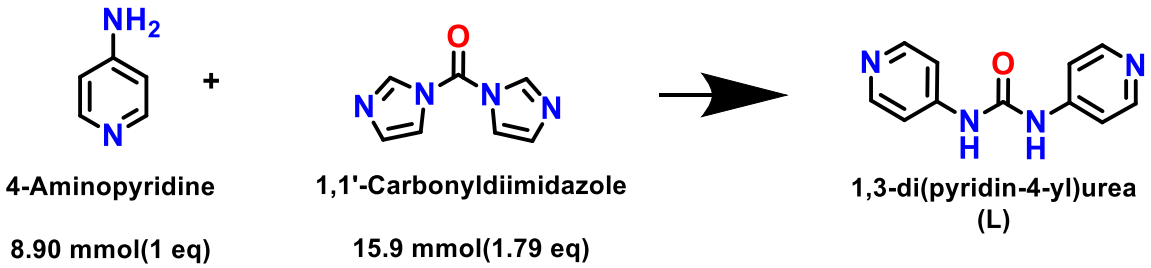

Scheme 2. Synthesis of linker ***L***.

4-Aminopyridine (1.50 g, 15.9 mmol, 1.79 eq) and 1,1'-Carbonyldiimidazole (1.44 g, 8.90 mmol, 1 eq) were dissolved in 200 ml toluene. The solution was left to reflux at 80°C for 3 hours under nitrogen environment. The heating was stopped and the reaction mixture was allowed to stir overnight at room temperature. The resulting white powder was obtained along the walls of round bottom flask. Powder was filtration and thoroughly washed with toluene, dichloromethane, water and finally with diethyl ether (60 ml). The product was dried at 60^0C under vacuum was characterised by NMR. ^{1}H NMR (DMSO-d^6): δ/ppm 7.44 (dd, 4H), 8.38 (dd, 4H), 9.30 (s, 2H); 13C NMR (DMSO-d^6): δ/ppm 112.57 (CH), 146.03 (C), 150.31 (CH), 151.85 (C)

(a)

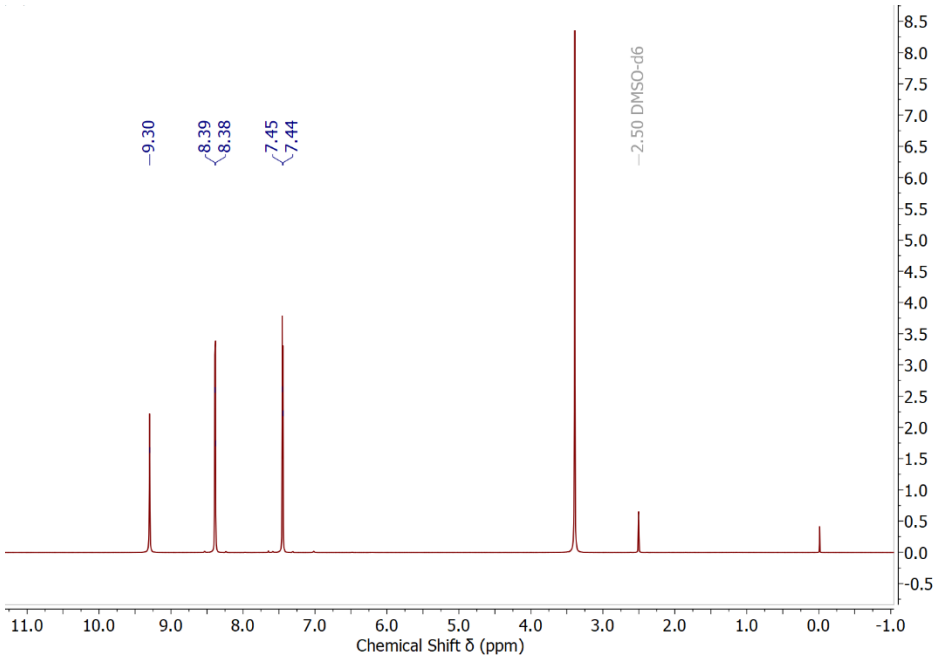

(b)

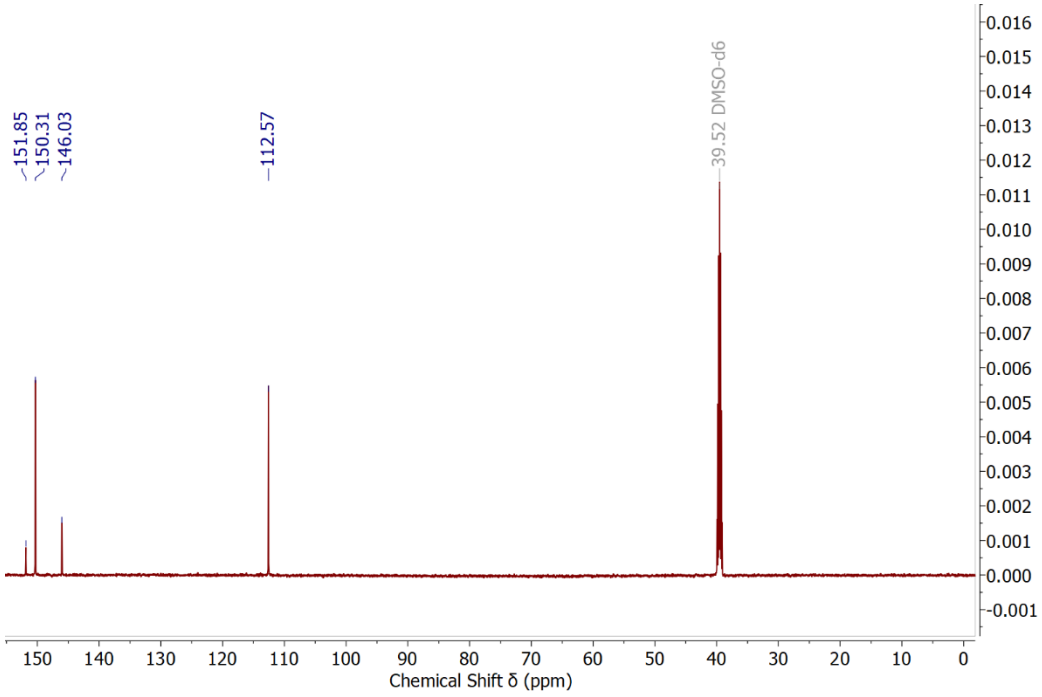

Figure S1. NMR spectra of 1,3-di(pyridin-4-yl)urea (*L*) (a) ^{1}H (b) ^{13}C.

Synthesis of CSMCRI-12

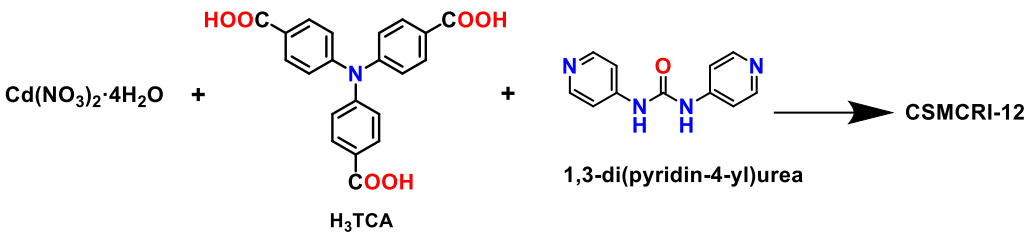

Scheme 3. Synthesis of **CSMCRI-12.**

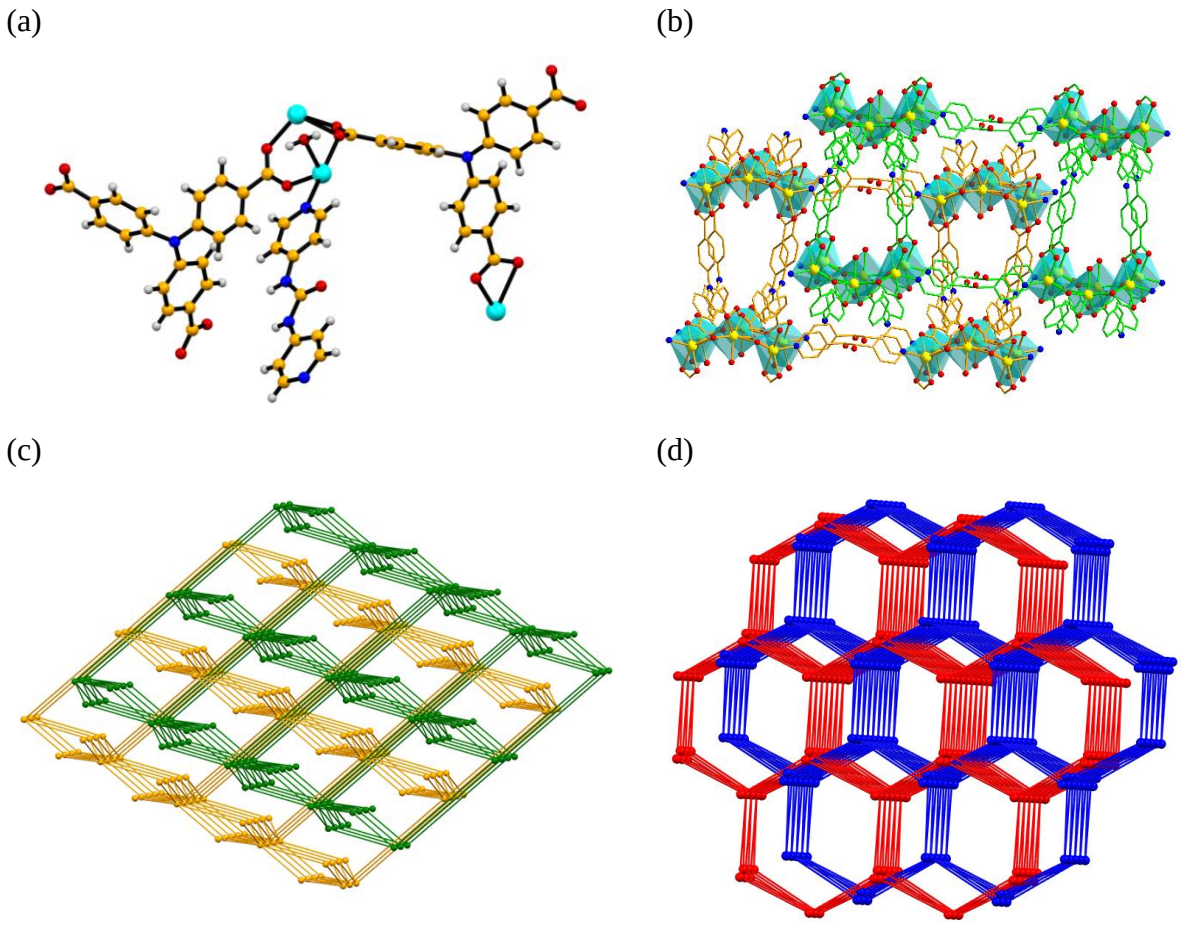

Figure S2. (a) Asymmetric unit of **CSMCRI-12**, (b) Representation of isostructural MOF **CSMCRI-9**, and (c), (d) Different topological representation two-fold interpenetrated pillar-bilayer framework**.**

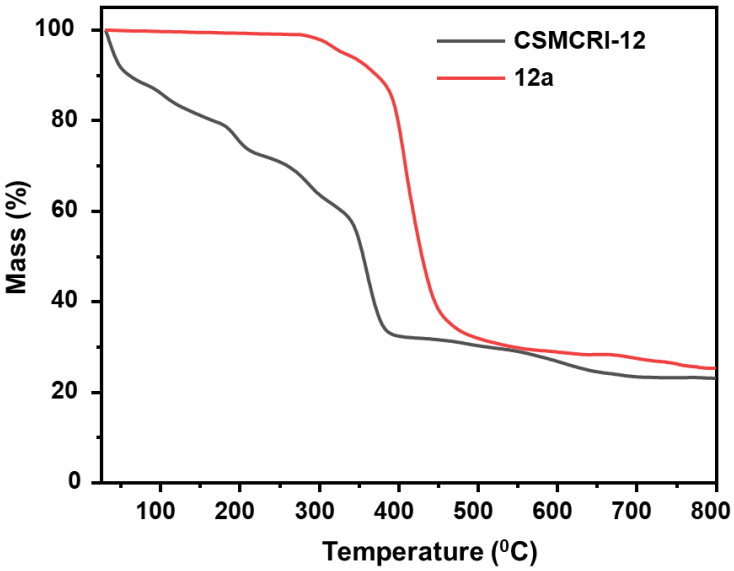

Figure S3. Thermogravimetric curve of **CSMCRI-12** and **12a**.

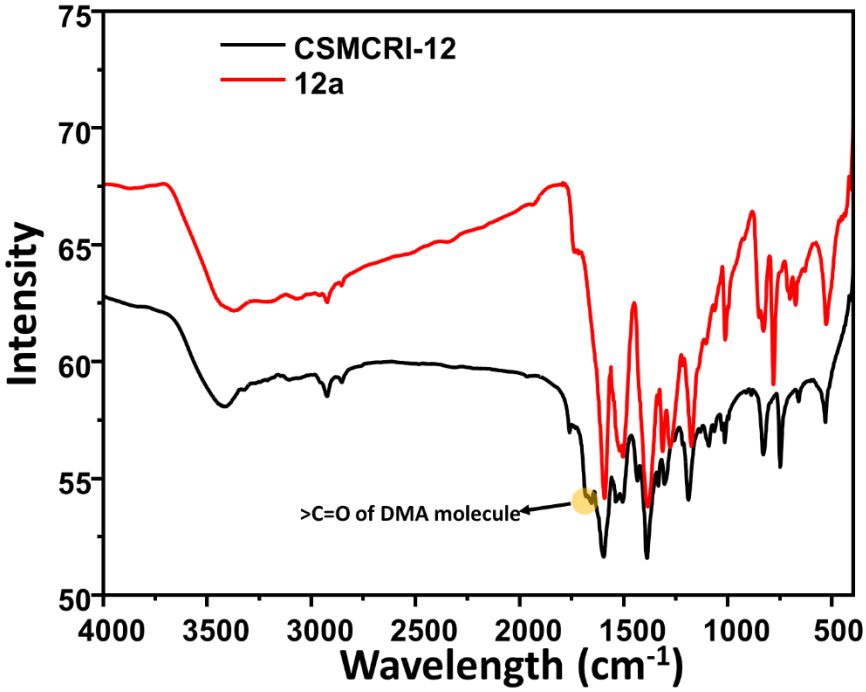

Figure S4. FT-IR spectra of **CSMCRI-12** and **12a**.

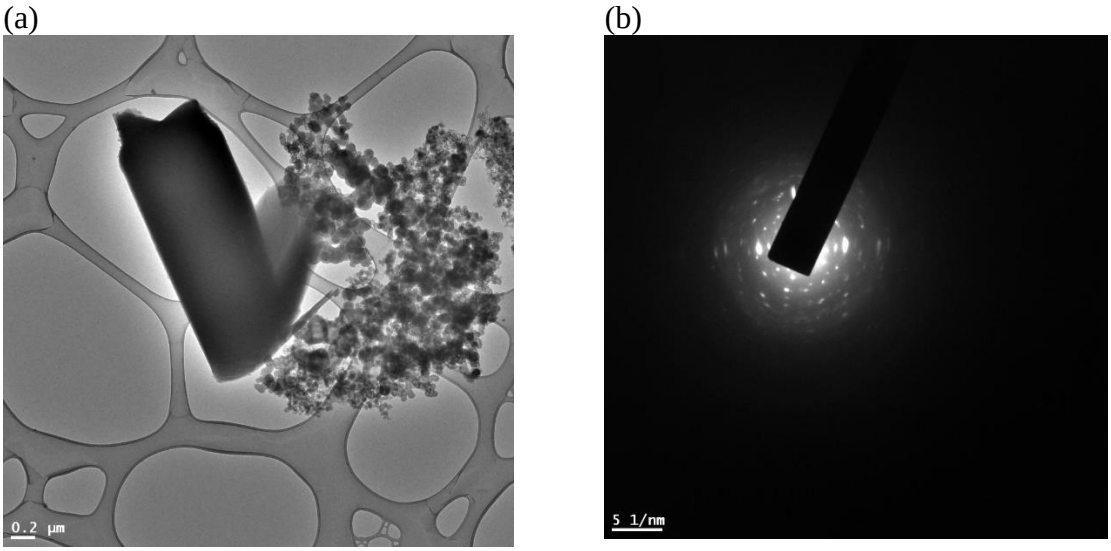

Figure S5. (a) TEM image of **CSMCRI-12** and (b) SAED pattern of the crystal.

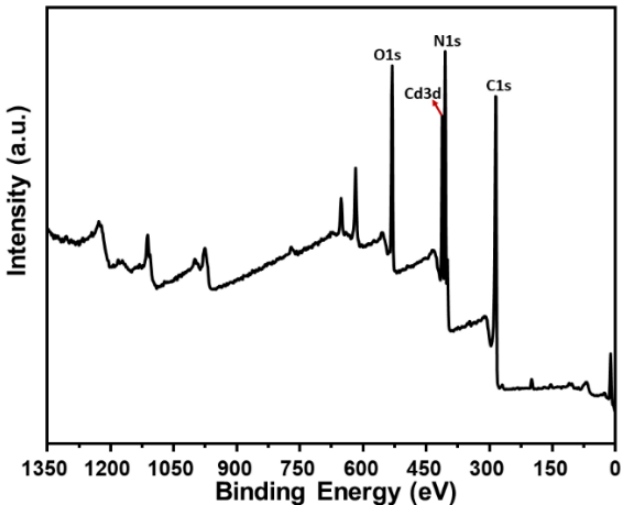

Figure S6. XPS survey spectra of the pristine framework.

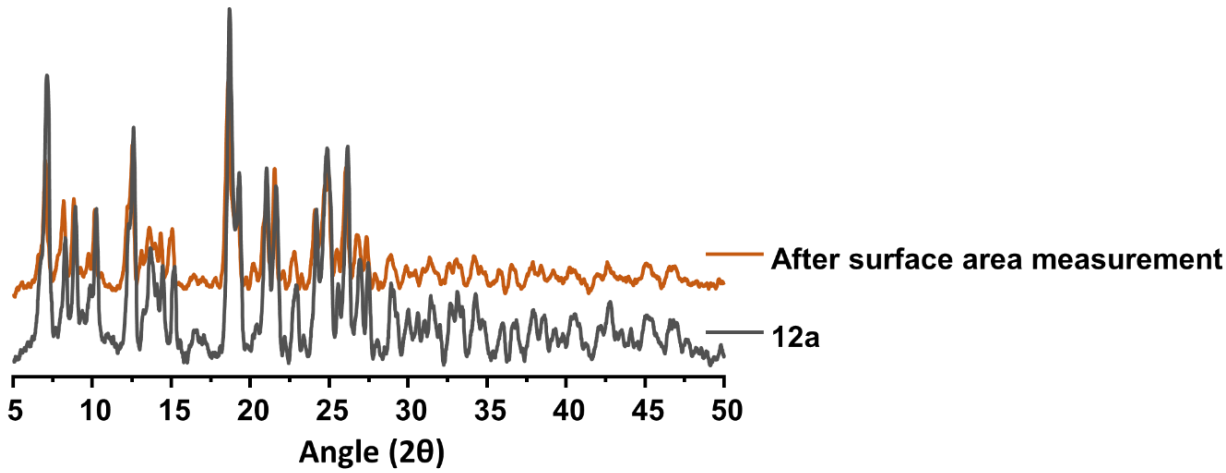

Figure S7. Comparative PXRD pattern of **12a** after surface area measurement.

Monitoring the progress of the reaction

Progress of the reaction was monitored by ^{1}H NMR spectroscopy through the integration of the α-vinyl and β-vinyl protons of β-nitrostyrene (δ 8.00−8.06 ppm) and the resulting aliphatic proton of the product 3-(2-nitro 1-phenylethyl)-^{1}H- indole (δ 4.92−5.25 ppm). So as to perform the catalyst recycling test, the used catalyst (separated by centrifugation) was washed with acetone and dried at 100 ^{0}C for 5 h under vacuum. Regenerated material was used further to perform the catalytic experiment and procedure was repeated for next 5 cycles.

Calculation of the % conversion

Total amount of complex = unreacted β-nitrostyrene + 3-(2-nitro-1-phenylethyl)-^{1}H-indole = 1+ 0.45 = 1.45

Percentage of the unreacted β-nitrostyrene: (100/1.45)% = 69%

Conversion of β-nitrostyrene = (100-69)% = 31%.

NMR Supporting Information

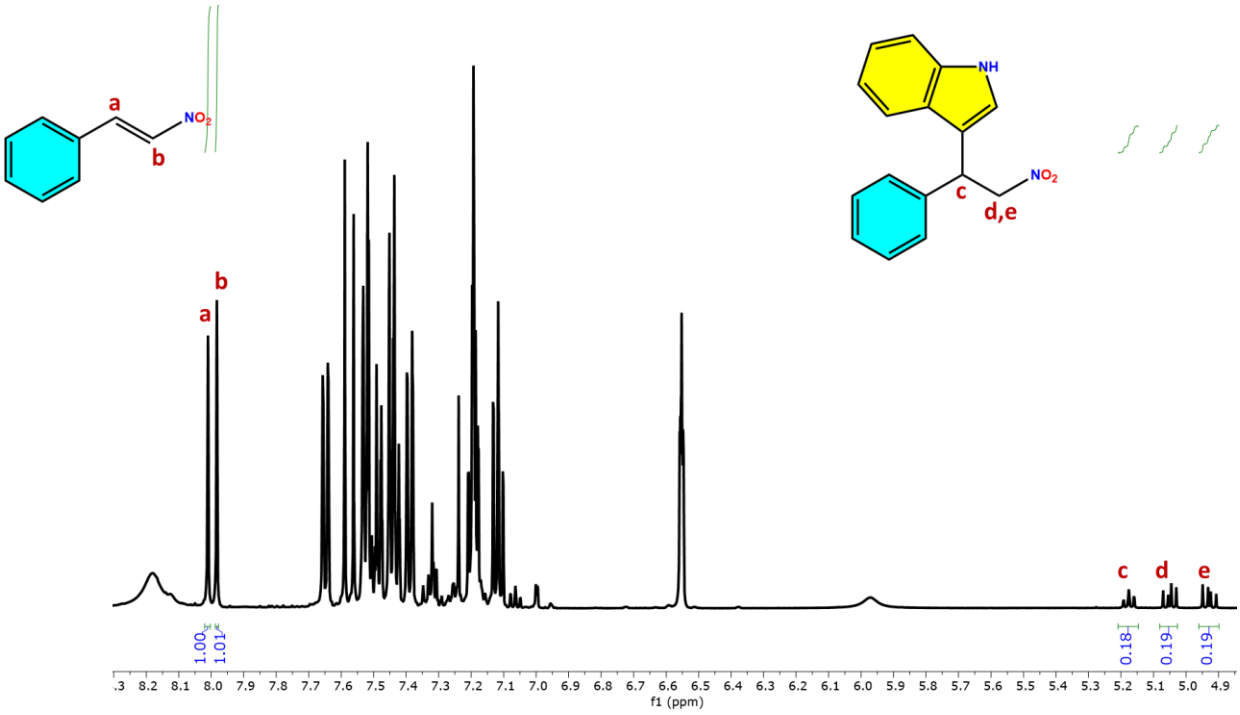

Figure S8. Integration in the ^{1}H NMR spectrum for the determination of conversion (%) of the reaction product catalyzed by **12a** (Table 1, entry 1).

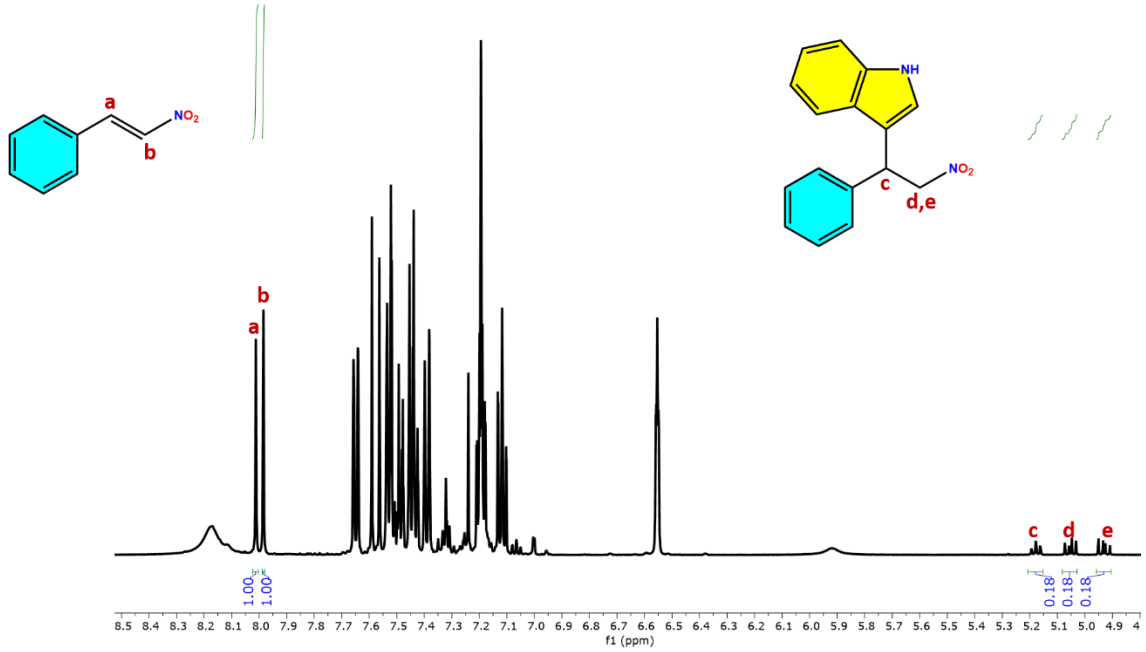

Figure S9. Integration in the ^{1}H NMR spectrum for the determination of conversion (%) of the reaction product catalyzed by **12a** (Table 1, entry 2).

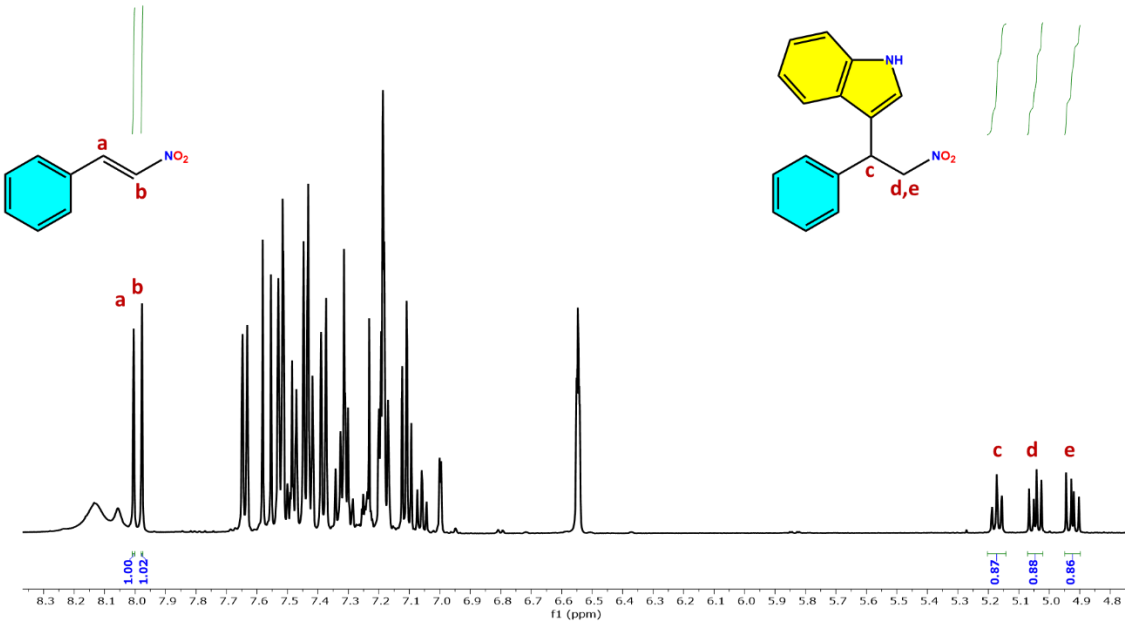

Figure S10. Integration in the ^{1}H NMR spectrum for the determination of conversion (%) of the reaction product catalyzed by **12a** (Table 1, entry 3).

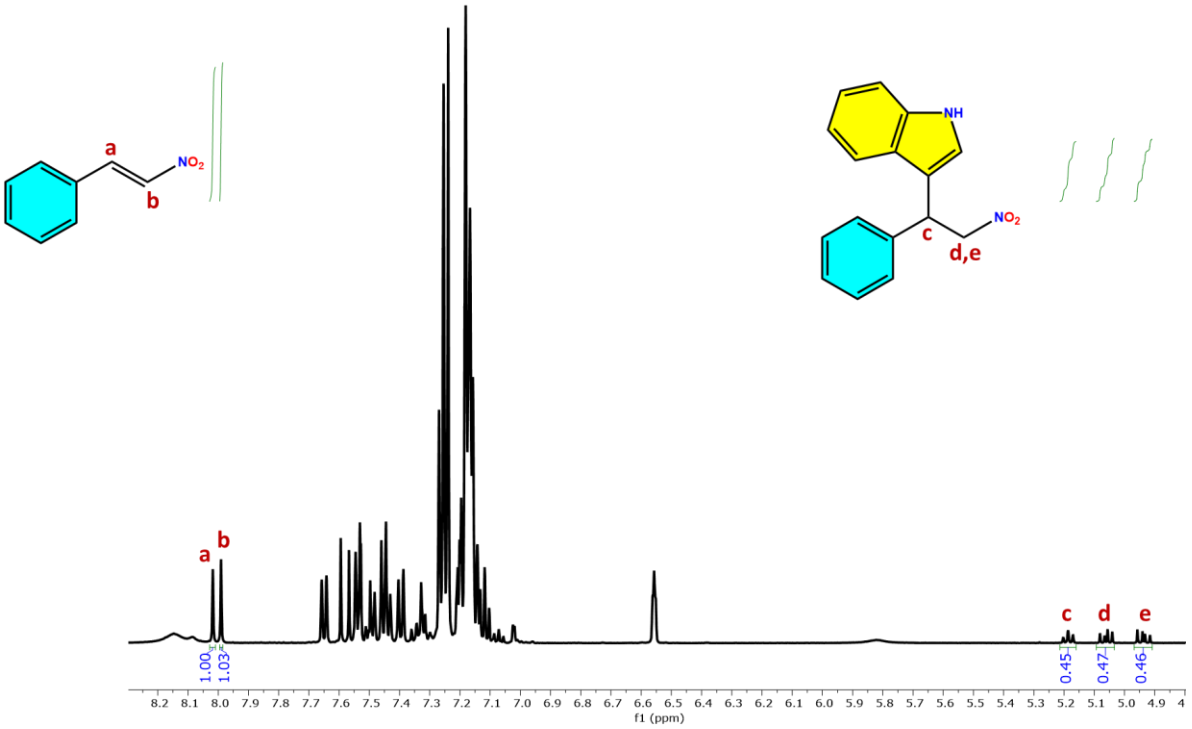

Figure S11. Integration in the ^{1}H NMR spectrum for the determination of conversion (%) of the reaction product catalyzed by **12a** (Table 1, entry 6).

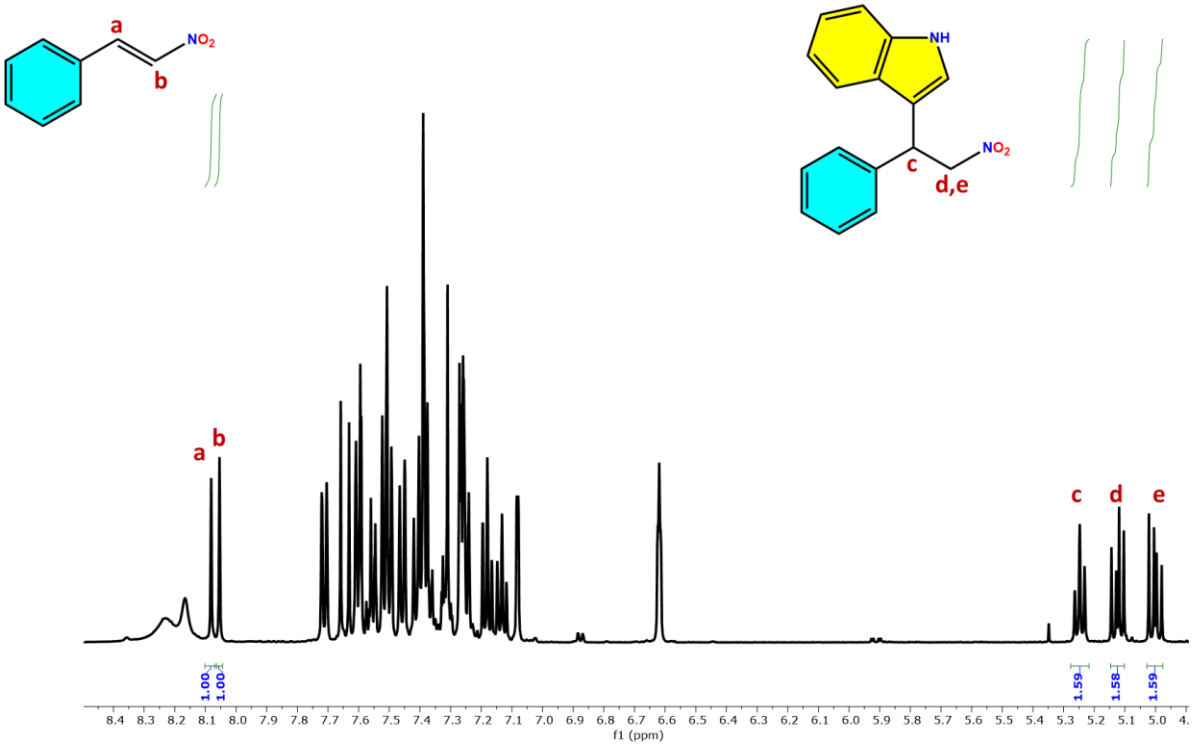

Figure S12. Integration in the 1H NMR spectrum for the determination of conversion (%) of the reaction product catalyzed by **12a** (Table 1, entry 7).

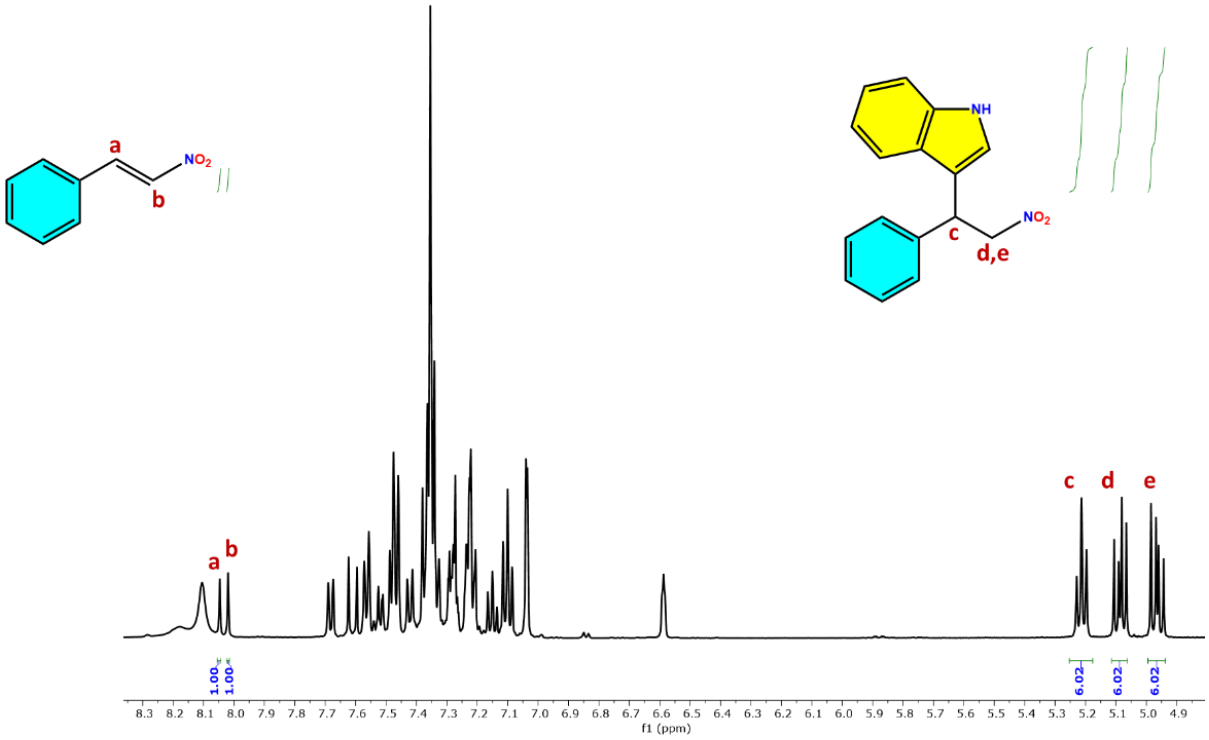

Figure S13. Integration in the ^{1}H NMR spectrum for the determination of conversion (%) of the reaction product catalyzed by **12a** (Table 1, entry 8).

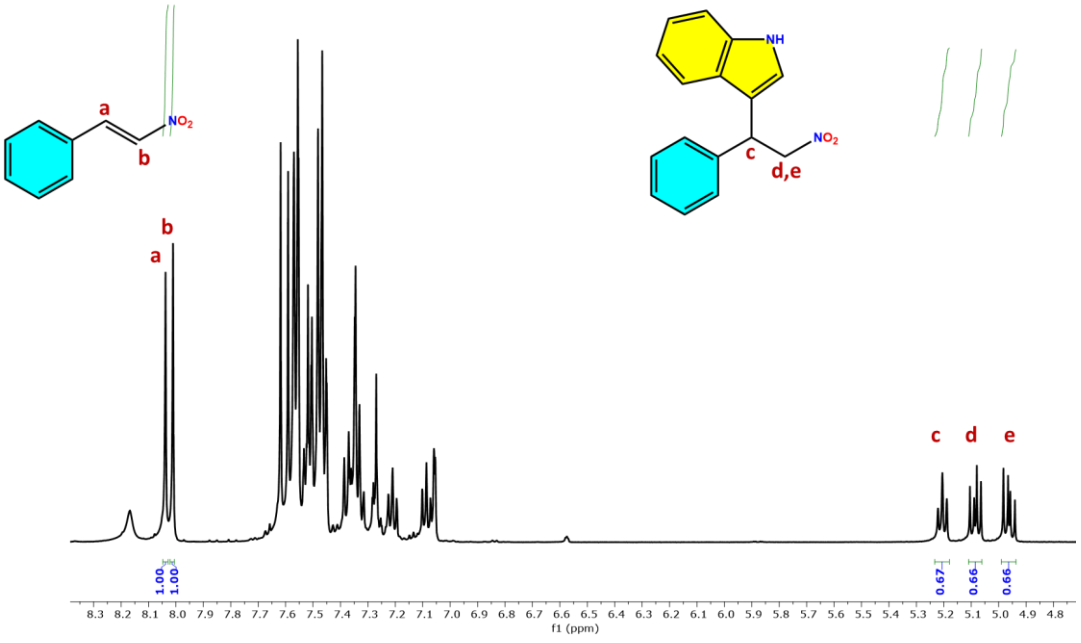

Figure S14. Integration in the ^{1}H NMR spectrum for the determination of conversion (%) of the reaction product catalyzed by $Cd(NO_3)_2 \cdot 4H_2O$ (Table 1, entry 10).

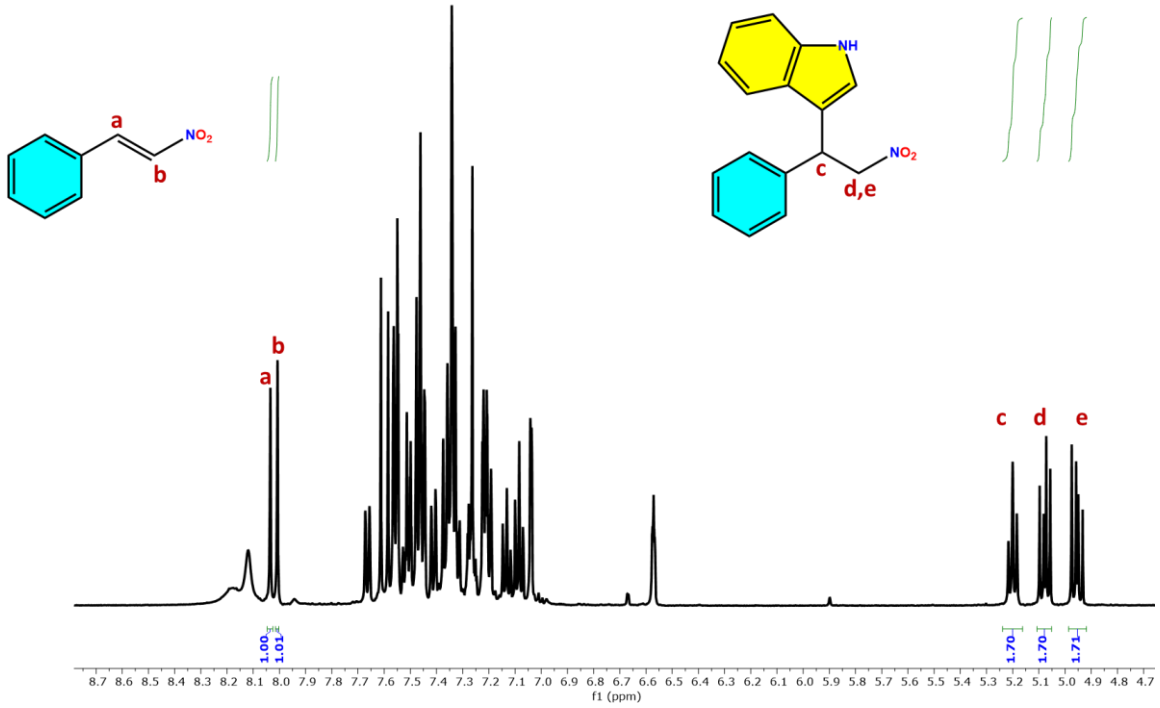

Figure S15. Integration in the ^{1}H NMR spectrum for the determination of conversicon (%) of the reaction product catalyzed by ***L*** (Table 1, entry 11).

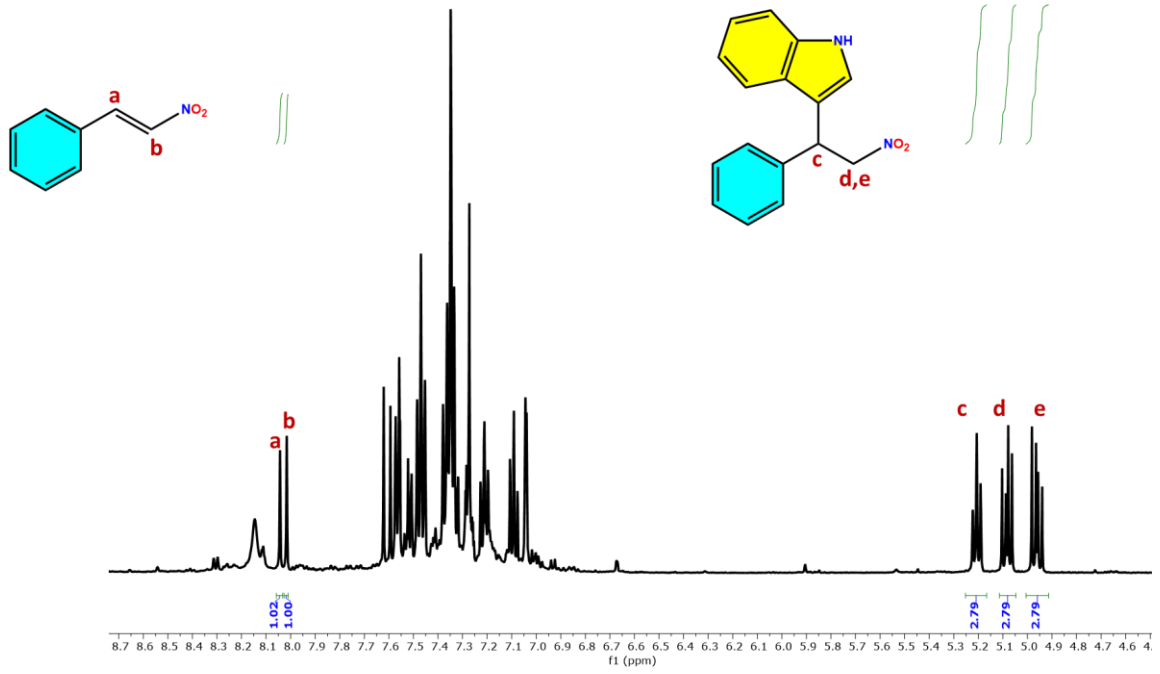

Figure S16. Integration in the ^{1}H NMR spectrum for the determination of conversion (%) of the reaction product catalyzed by ***L***/$Cd(NO_3)_2 \cdot 4H_2O$ (Table 1, entry 12).

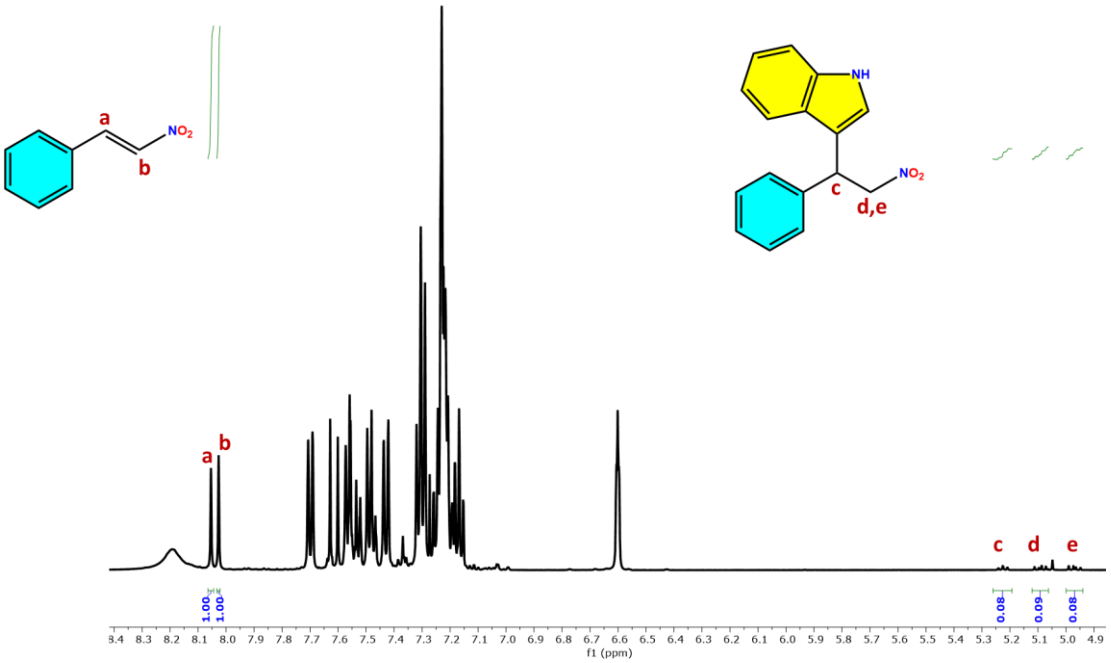

Figure S17. Integration in the ^{1}H NMR spectrum for the determination of conversion (%) of the reaction product catalyzed by H_3TCA (Table 1, entry 13).

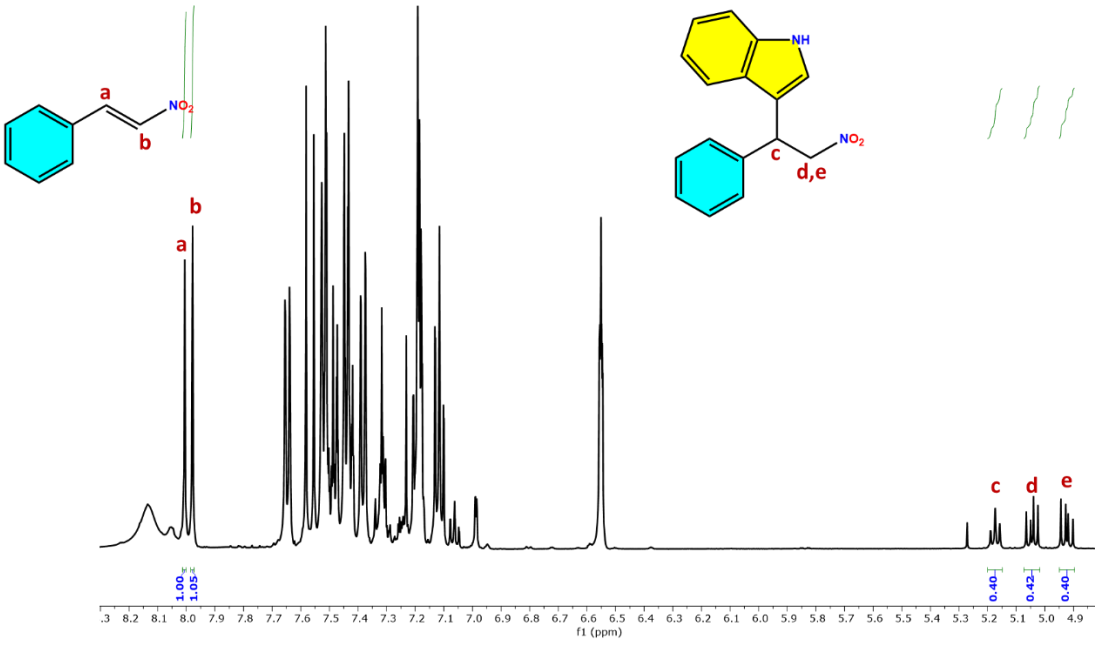

Figure S18. Integration in the ^{1}H NMR spectrum for the determination of conversion (%) of the reaction product catalyzed by **CSMCRI-12** (Table 1, Entry 14).

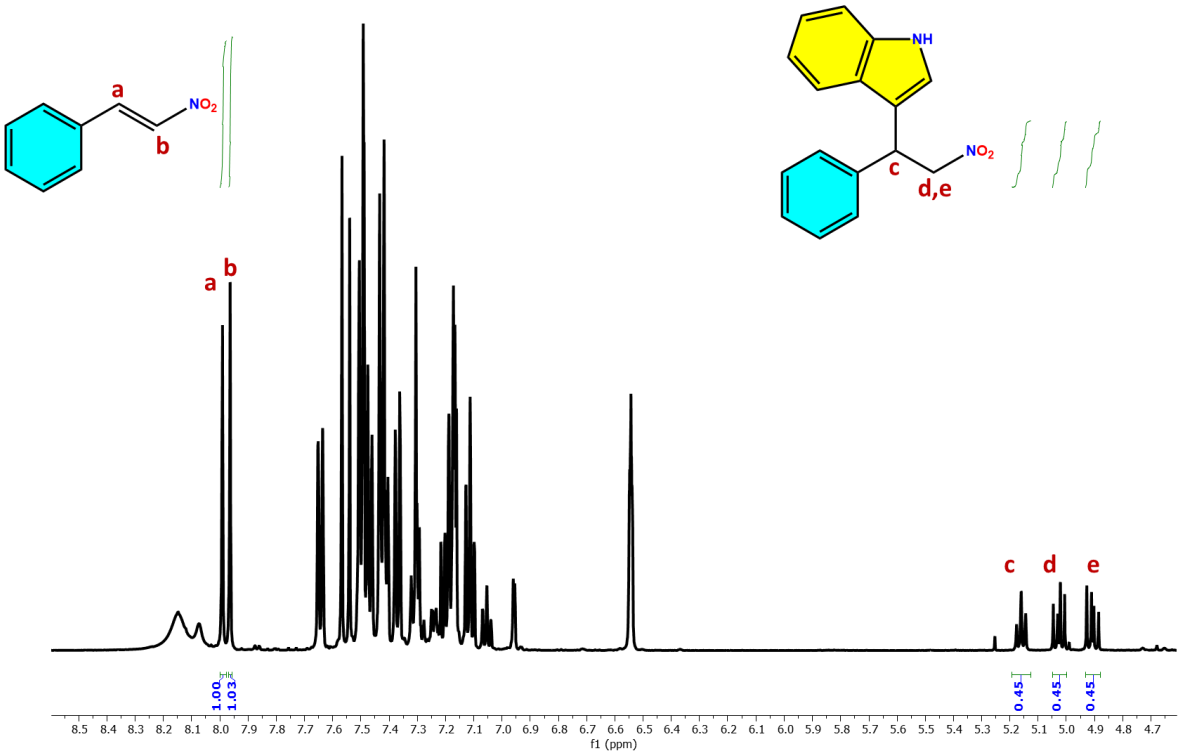

Figure S19 Integration in the ^{1}H NMR spectrum for the determination of conversion (%) of the reaction product catalyzed by activated **CSMCRI-9** (**9a**) (Table 1, entry 16).

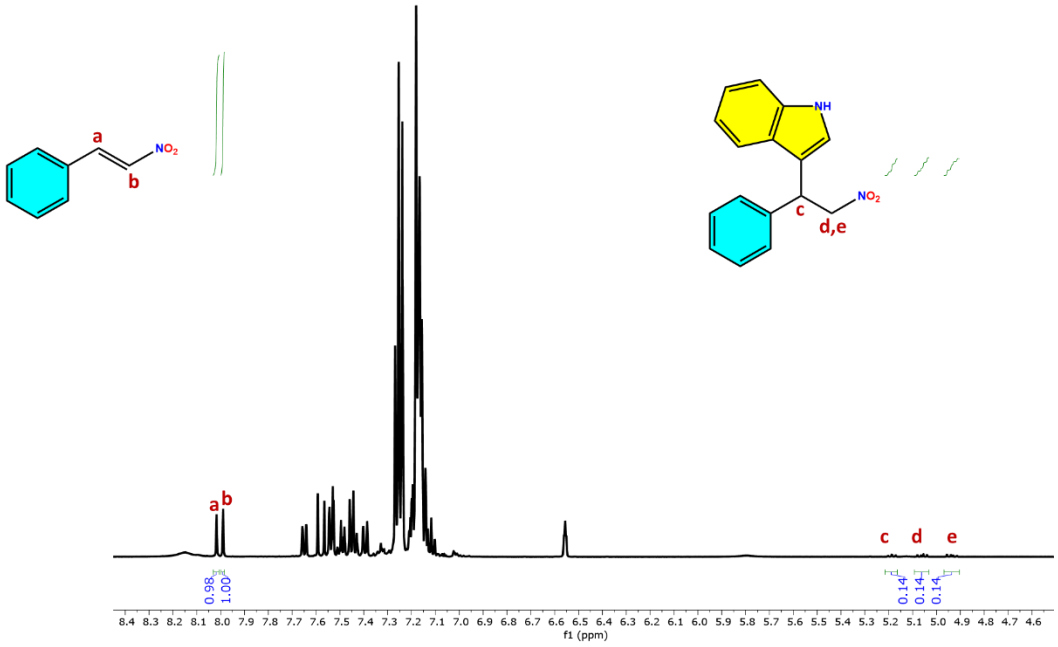

Figure S20. Integration in the ^{1}H NMR spectrum for the determination of conversion (%) of the reaction product catalyzed by **12a** (Solvent: chloroform, RT, **12a**: 10 mol%).

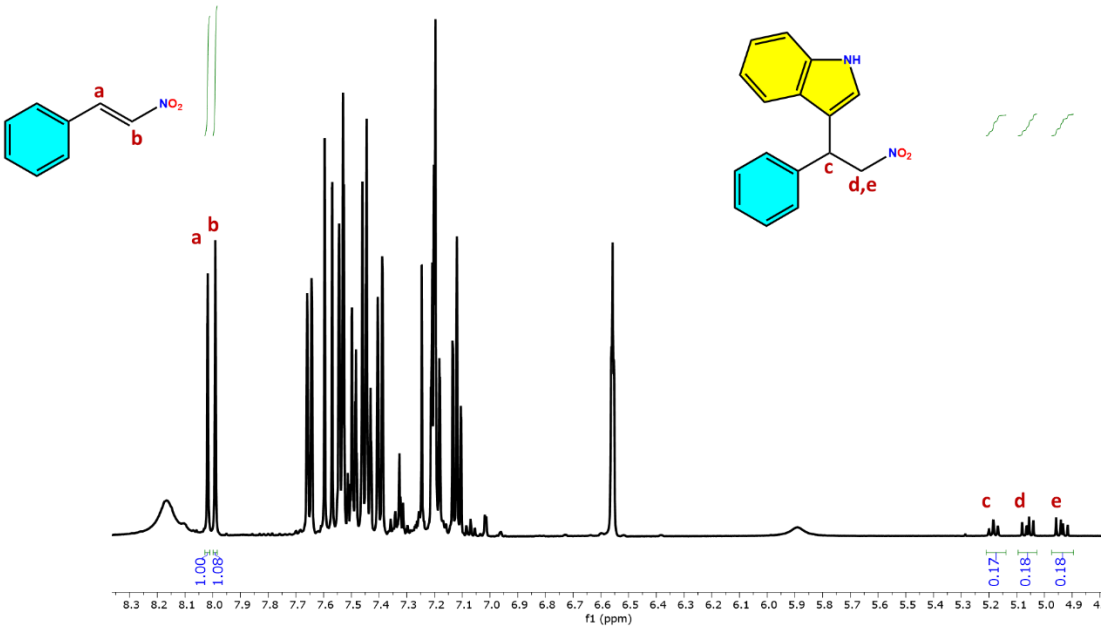

Figure S21. Integration in the ^{1}H NMR spectrum for the determination of conversion (%) of the reaction product catalyzed by **12a** (Solvent : acetonitrile, RT, **12a**: 10 mol%)

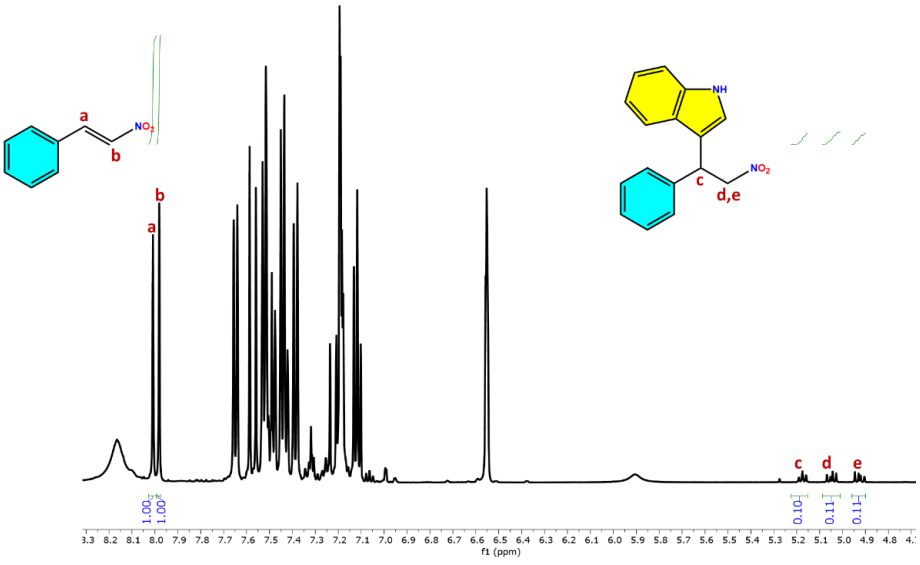

Figure S22. Integration in the ^{1}H NMR spectrum for the determination of conversion (%) of the reaction product catalyzed by **12a** (Solvent: dichloromethane, RT, **12a**: 10 mol%)

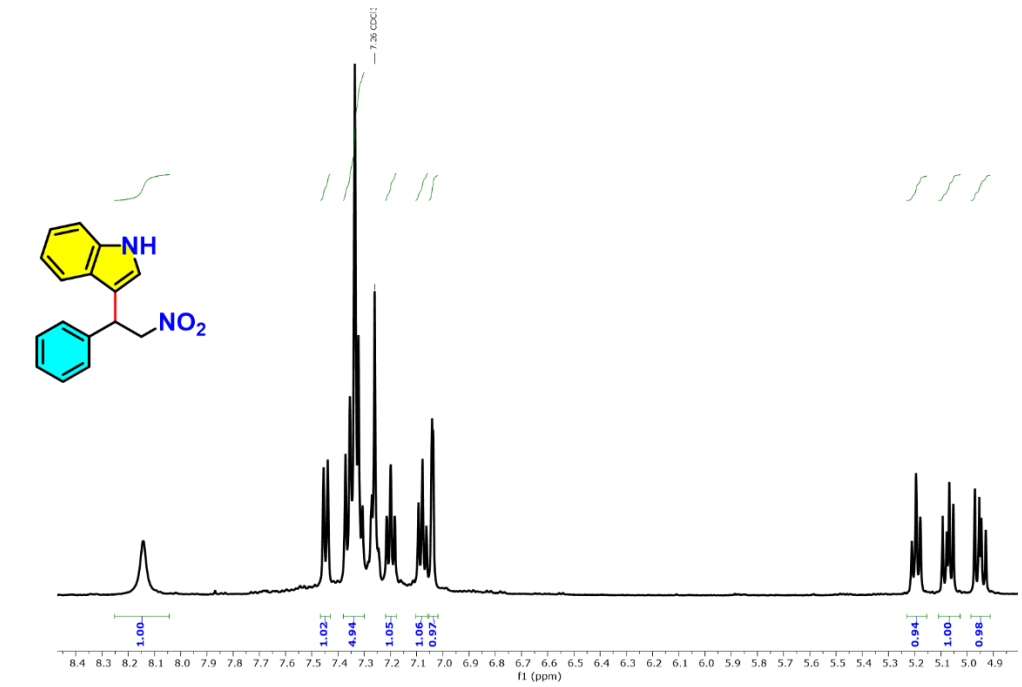

Figure S23. Integration in the ^{1}H NMR spectrum for the determination of conversion (%) of the reaction product catalyzed by **12a** (Table 2, entry 1).

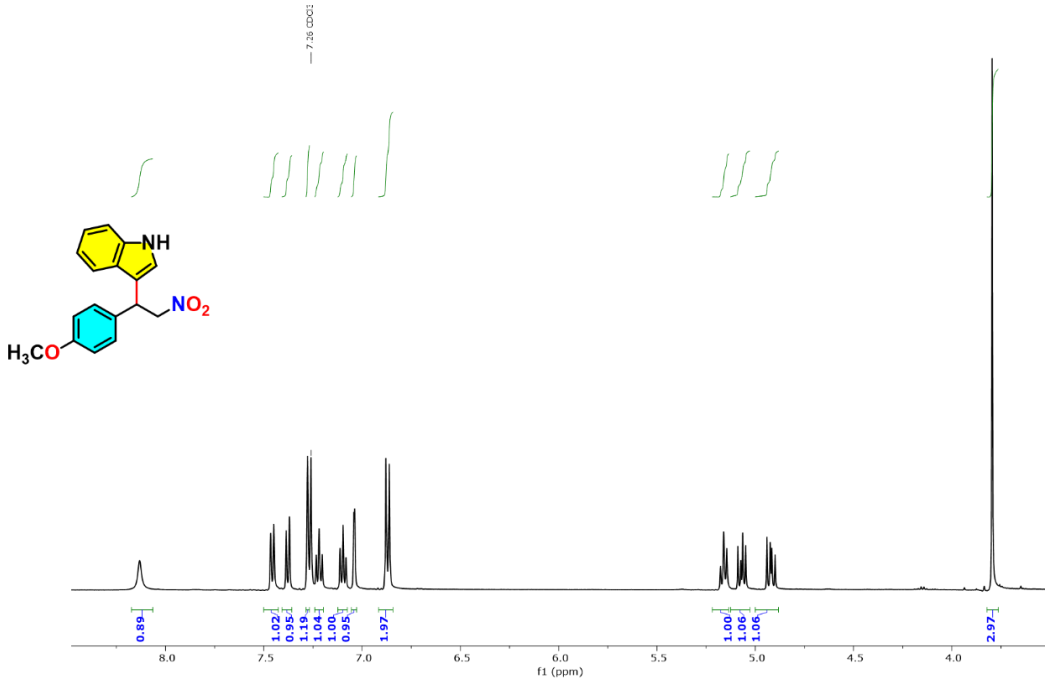

Figure S24. Integration in the ^{1}H NMR spectrum for the determination of conversion (%) of the reaction product catalyzed by **12a** (Table 2, entry 2).

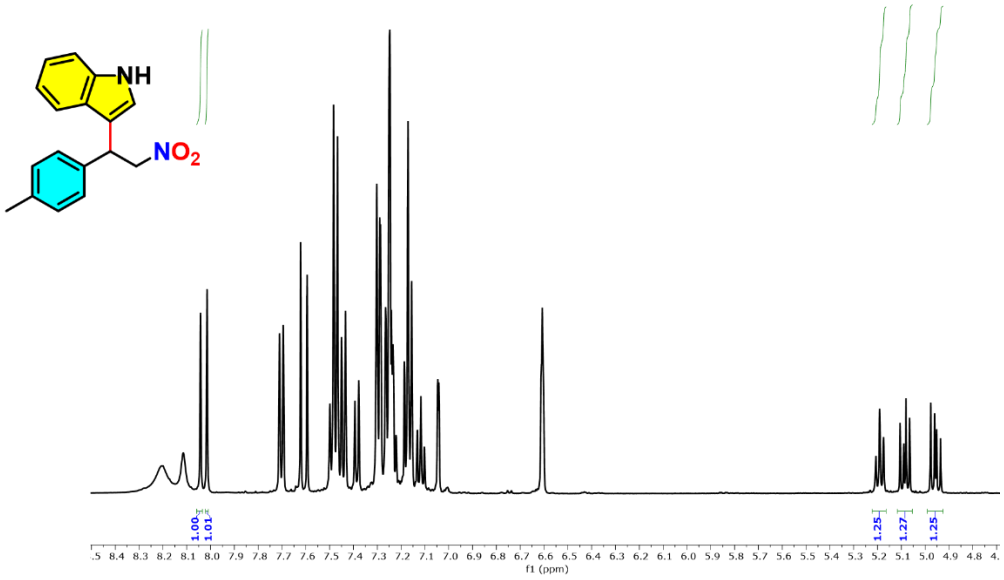

Figure S25. Integration in the ^{1}H NMR spectrum for the determination of conversion(%) of the reaction product catalyzed by **12a** (Table 2, entry 3).

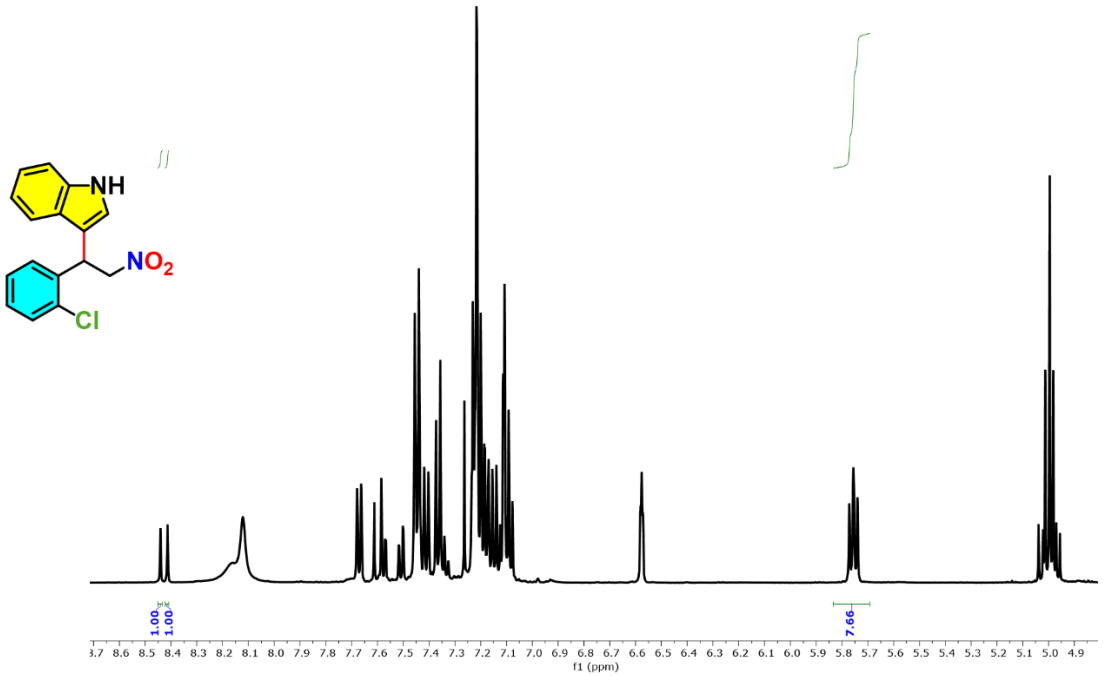

Figure S26. Integration in the ^{1}H NMR spectrum for the determination of conversion (%) of the reaction product catalyzed by **12a** (Table 2, entry 4).

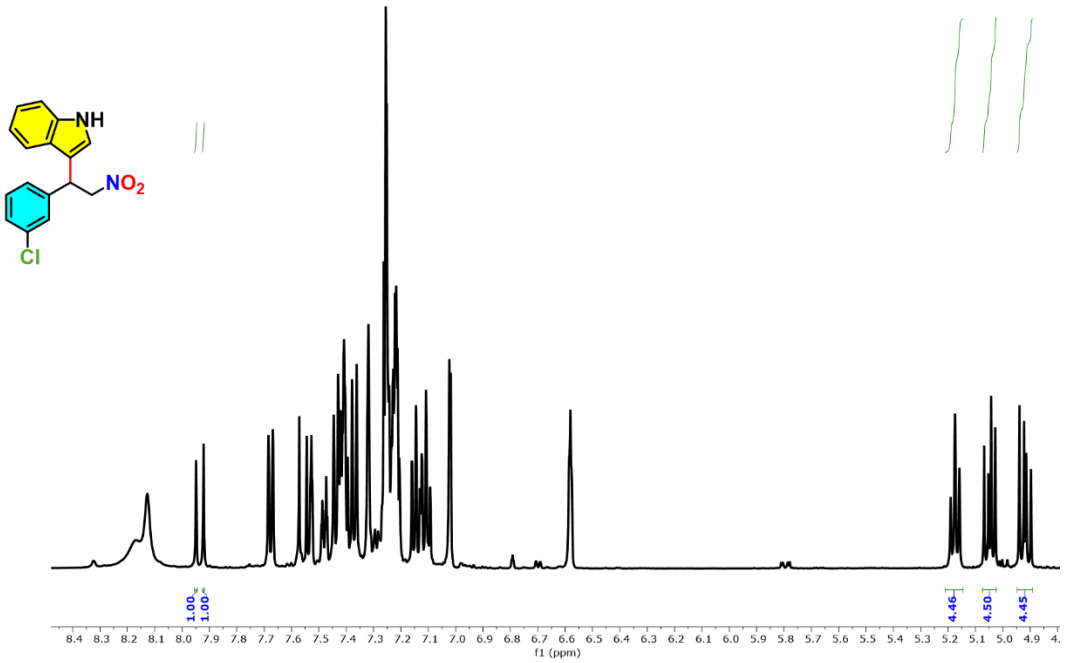

Figure S27. Integration in the ^{1}H NMR spectrum for the determination of conversion(%) of the reaction product catalyzed by **12a** (Table 2, entry 5).

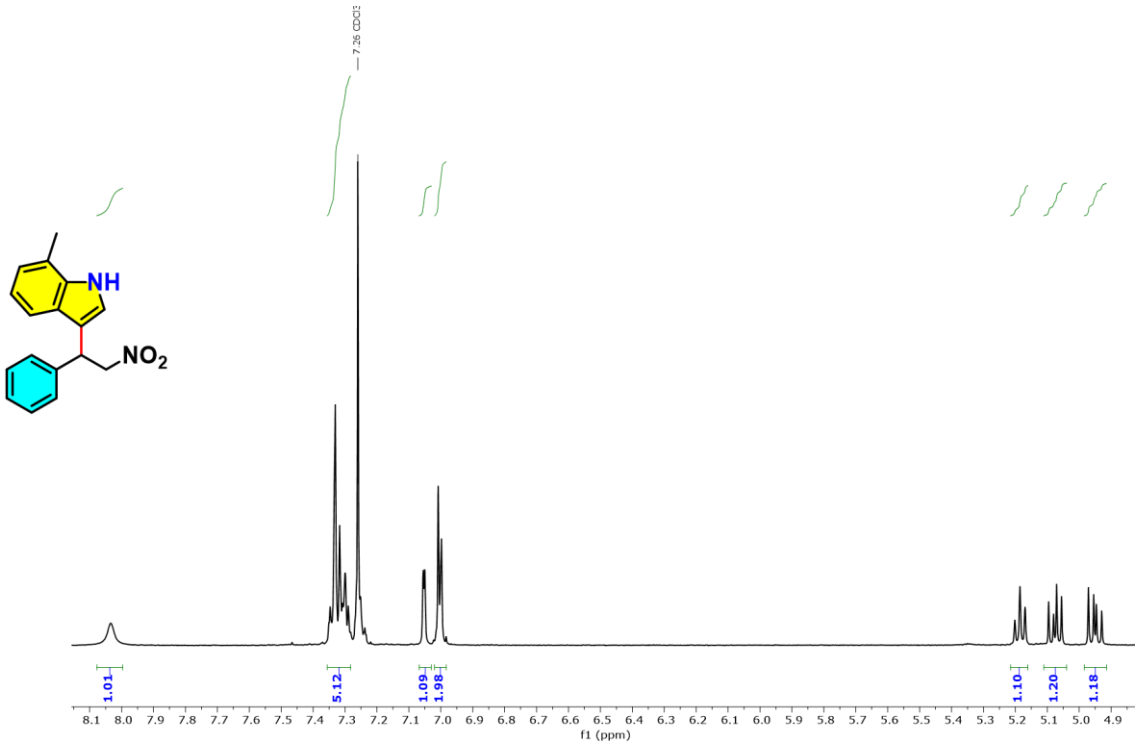

Figure S28. Integration in the ^{1}H NMR spectrum for the determination of conversion(%) of the reaction product catalyzed by **12a** (Table 2, entry 6).

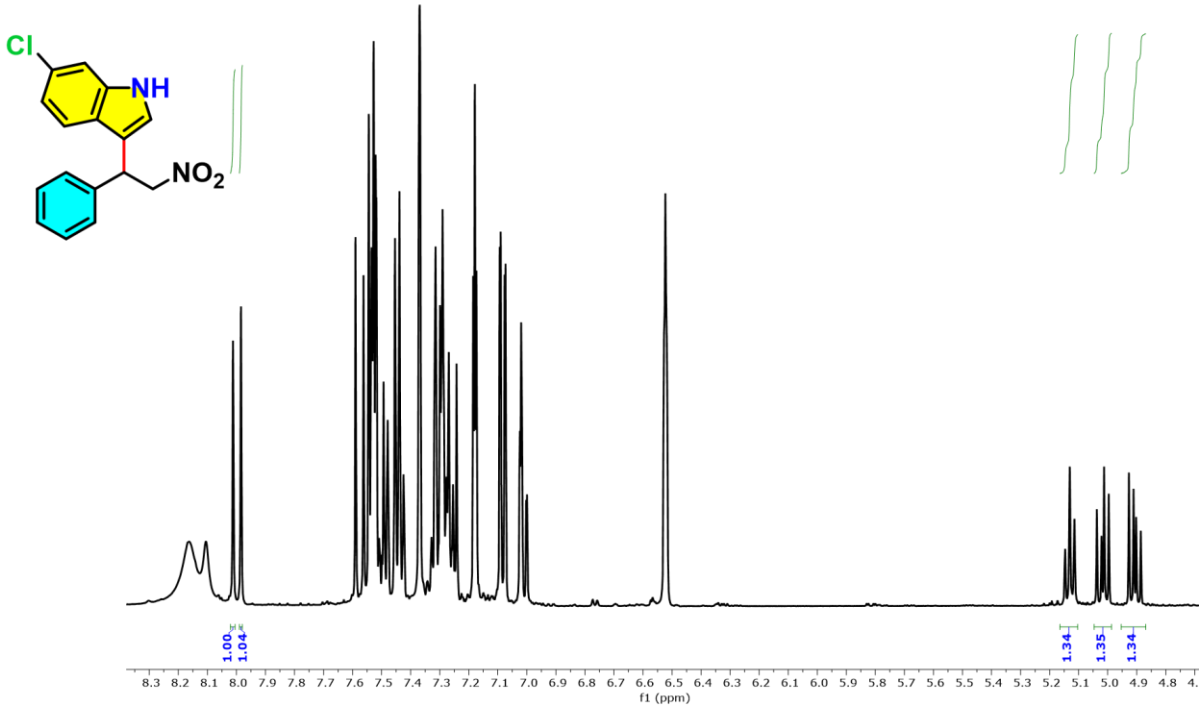

Figure S29. Integration in the ^{1}H NMR spectrum for the determination of conversion(%) of the reaction product catalyzed by **12a** (Table 2, entry 7).

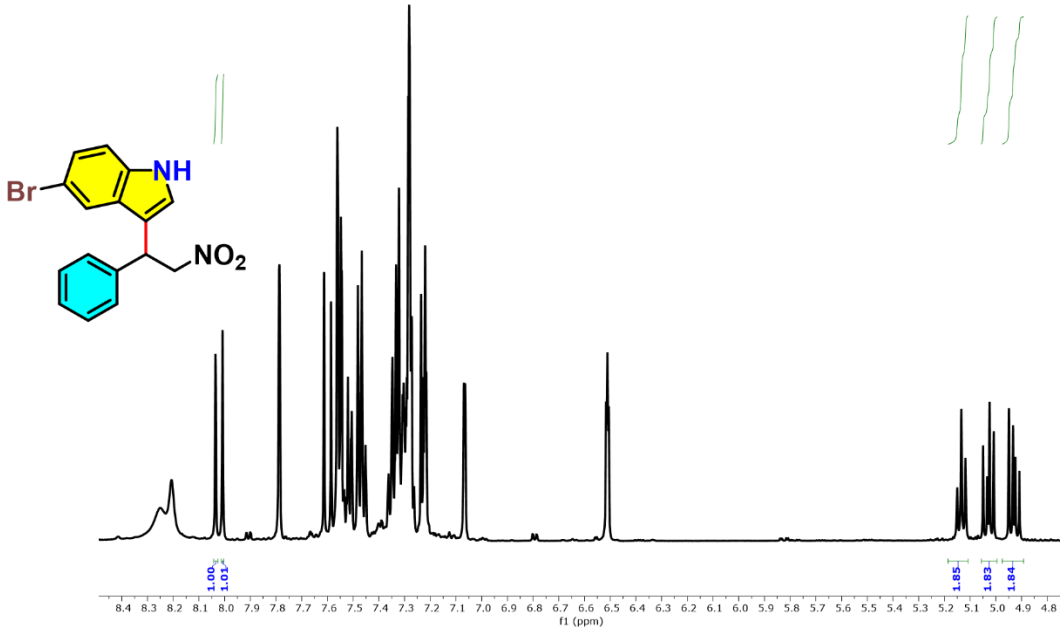

Figure S30. Integration in the ^{1}H NMR spectrum for the determination of conversion(%) of the reaction product catalyzed by **12a** (Table 2, entry 8).

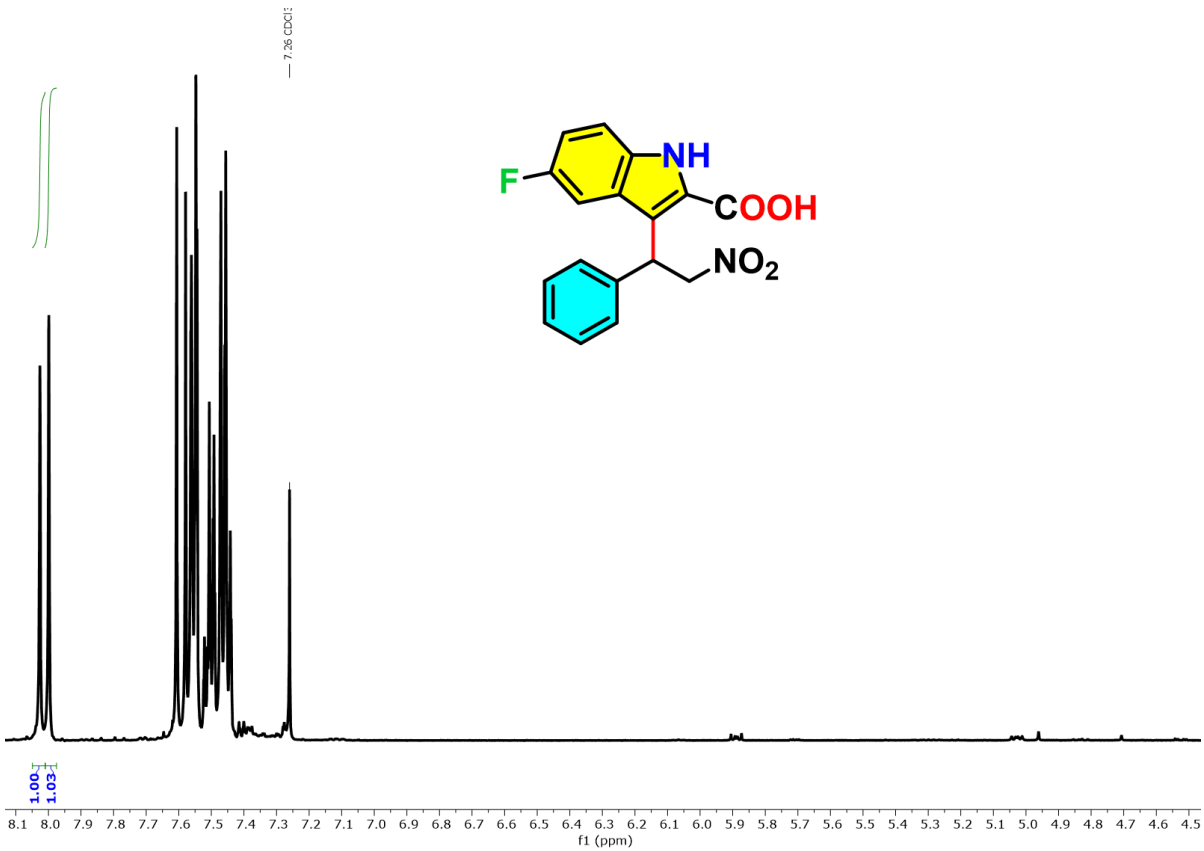

Figure S31. Integration in the ^{1}H NMR spectrum for the determination of conversion (%) of the reaction product catalyzed by **12a** (Table 2, entry 9).

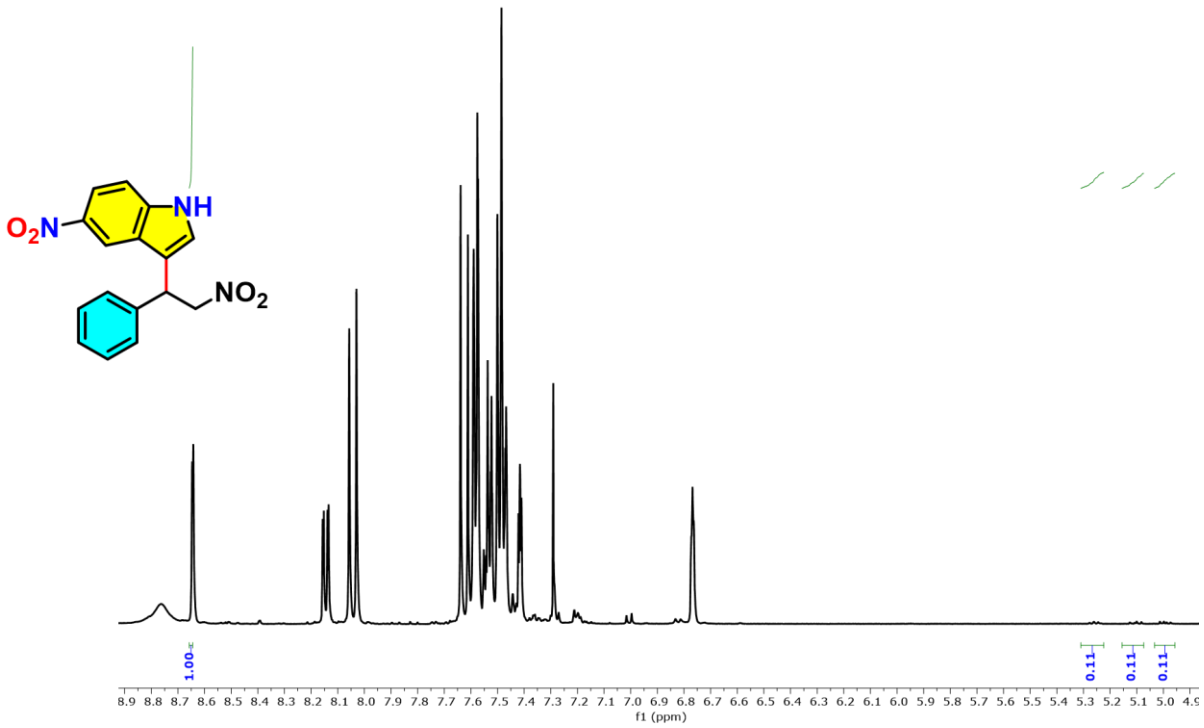

Figure S32. Integration in the ^{1}H NMR spectrum for the determination of conversion(%) of the reaction product catalyzed by **12a** (Table 2, entry 10).

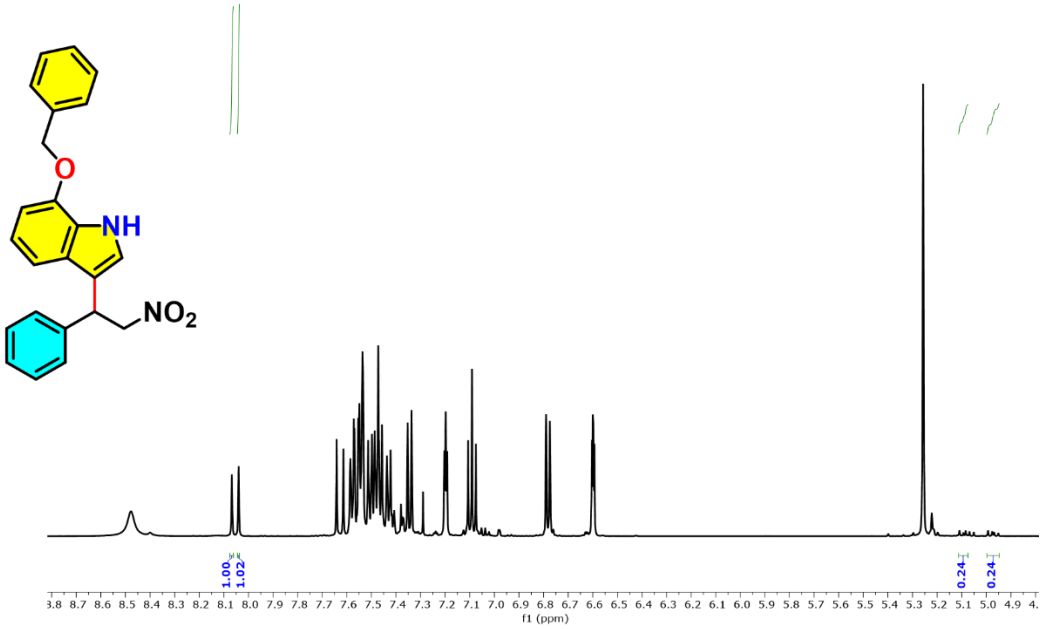

Figure S33. Integration in the ^{1}H NMR spectrum for the determination of conversion(%) of the reaction product catalyzed by **12a** (Table 2, entry 11).

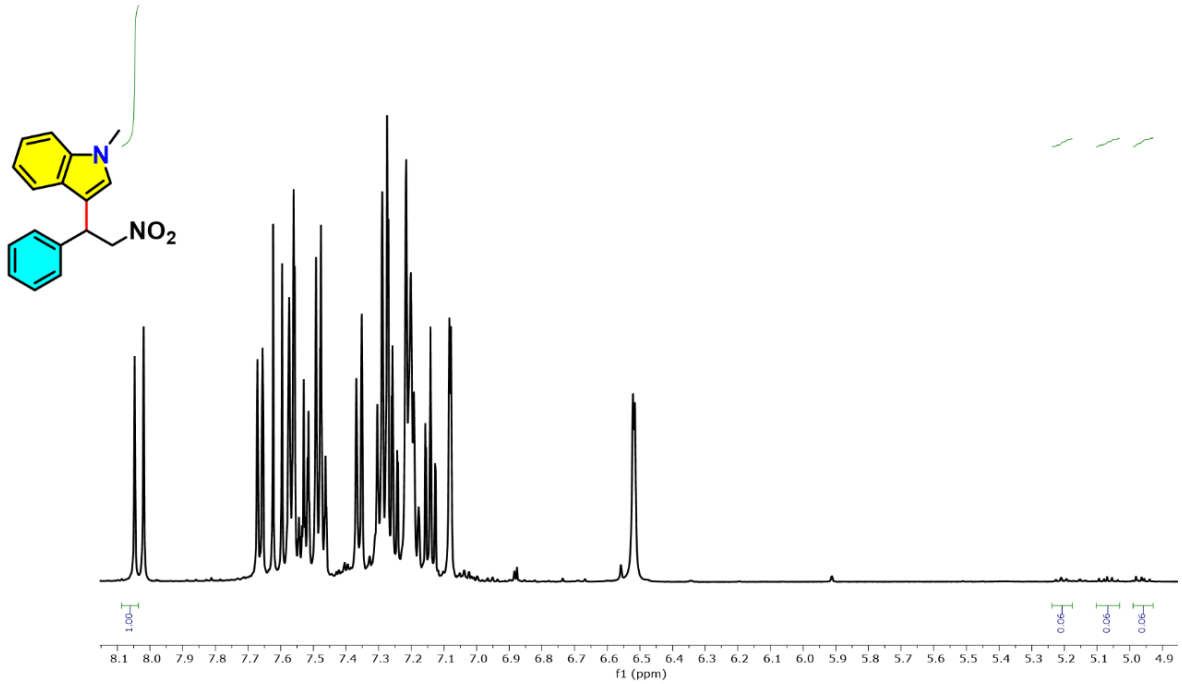

Figure S34. Integration in the ^{1}H NMR spectrum for the determination of conversion (%) of the reaction product catalyzed by **12a** (Table 2, entry 12).

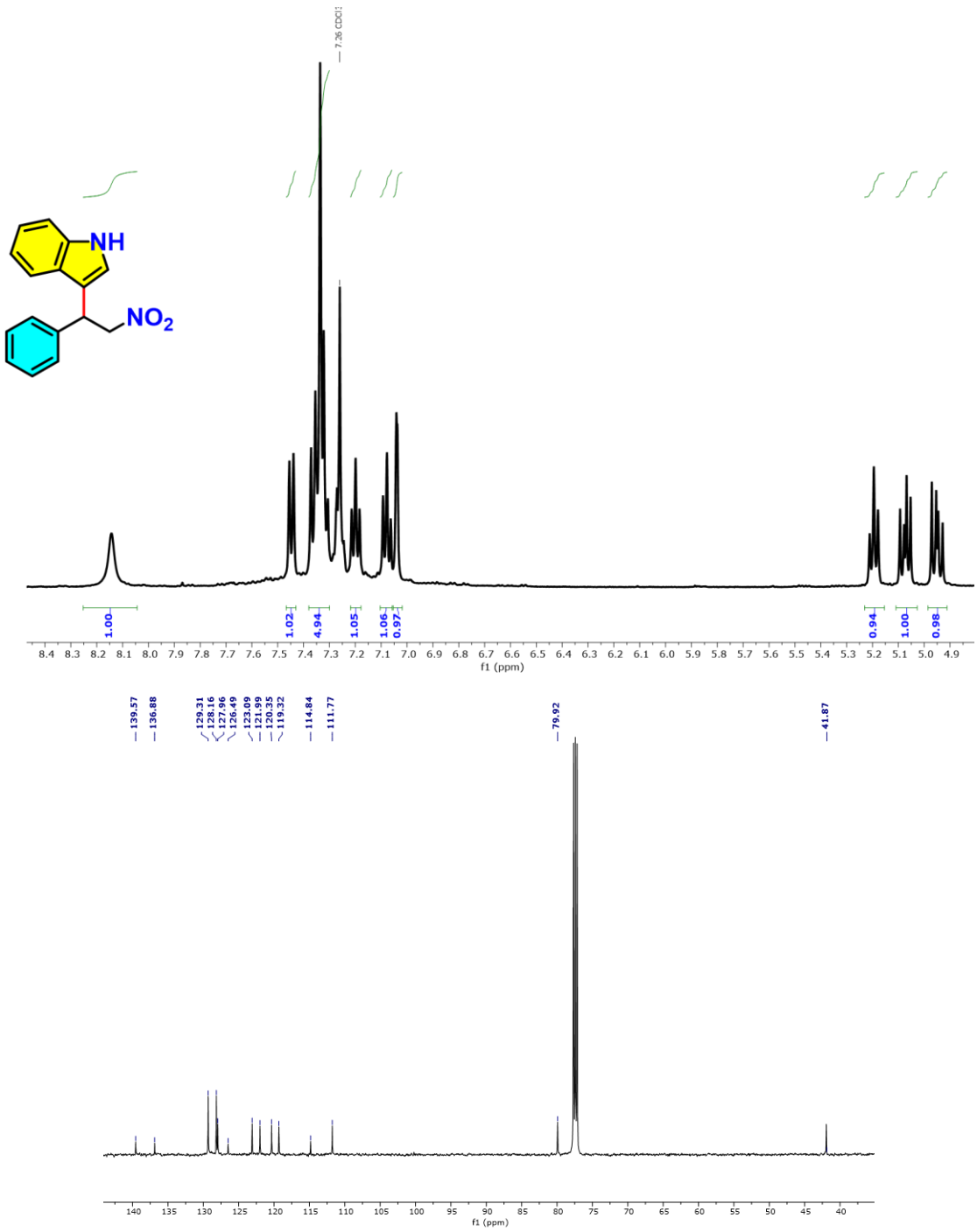

Figure S35. (a) ^{1}H and (b) ^{13}C NMR (Table 2, entry 1) of substrate scope 3-(2-nitro-1-phenylethyl)-1H-indole.

(a)

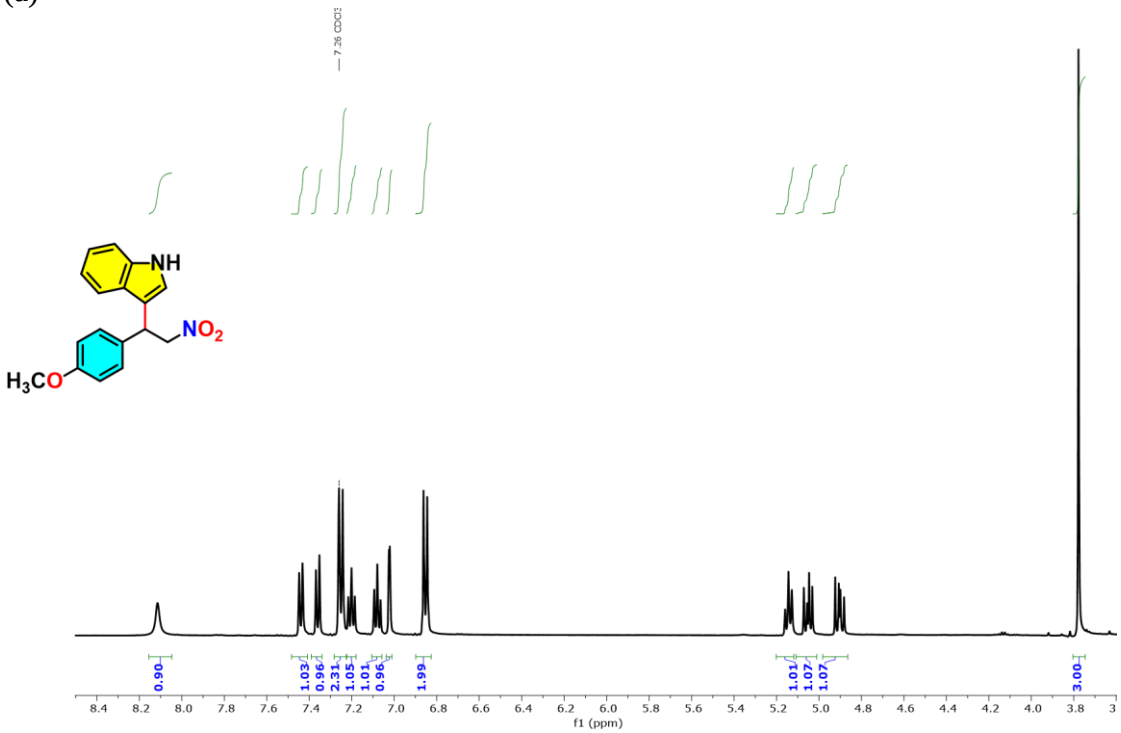

(b)

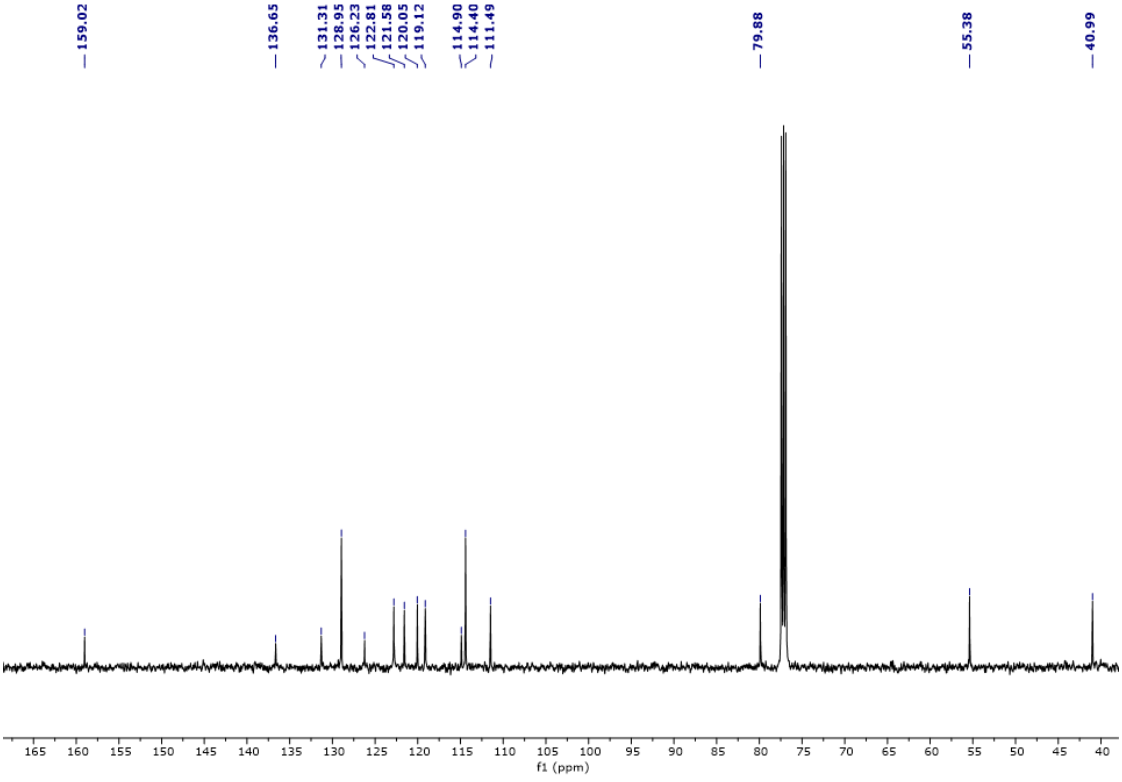

Figure S36. (a)^{1}H and (b) ^{13}C NMR spectra (Table 2, entry 2) of substrate scope 3-(1-(4-methoxyphenyl)-2-nitroethyl)-1H-indole**.**

(a)

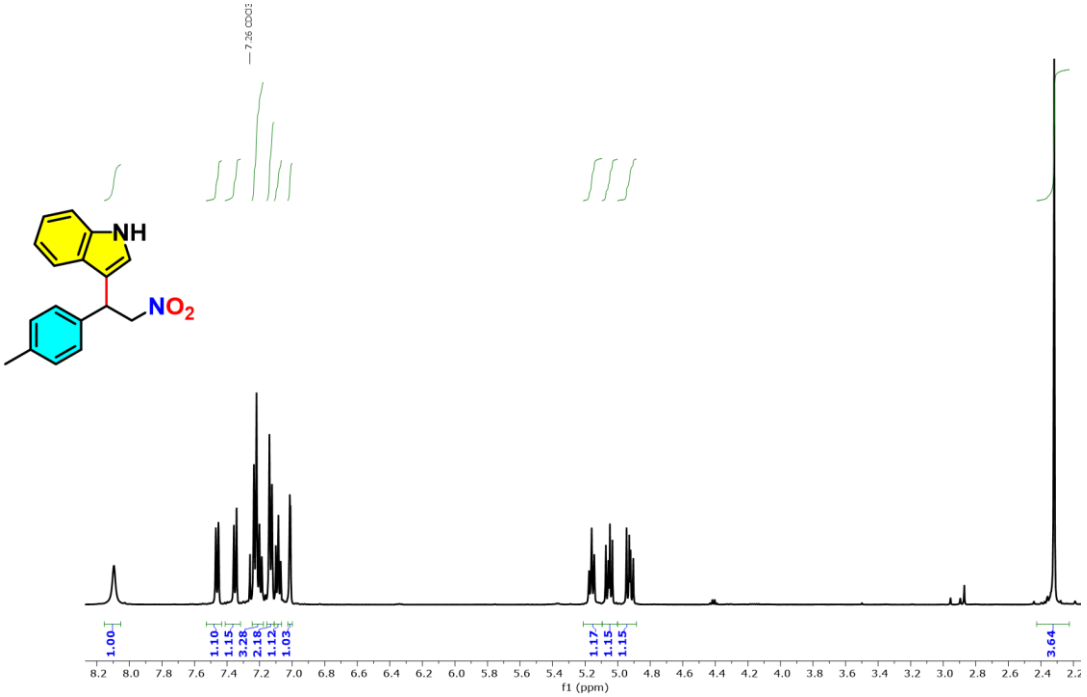

(b)

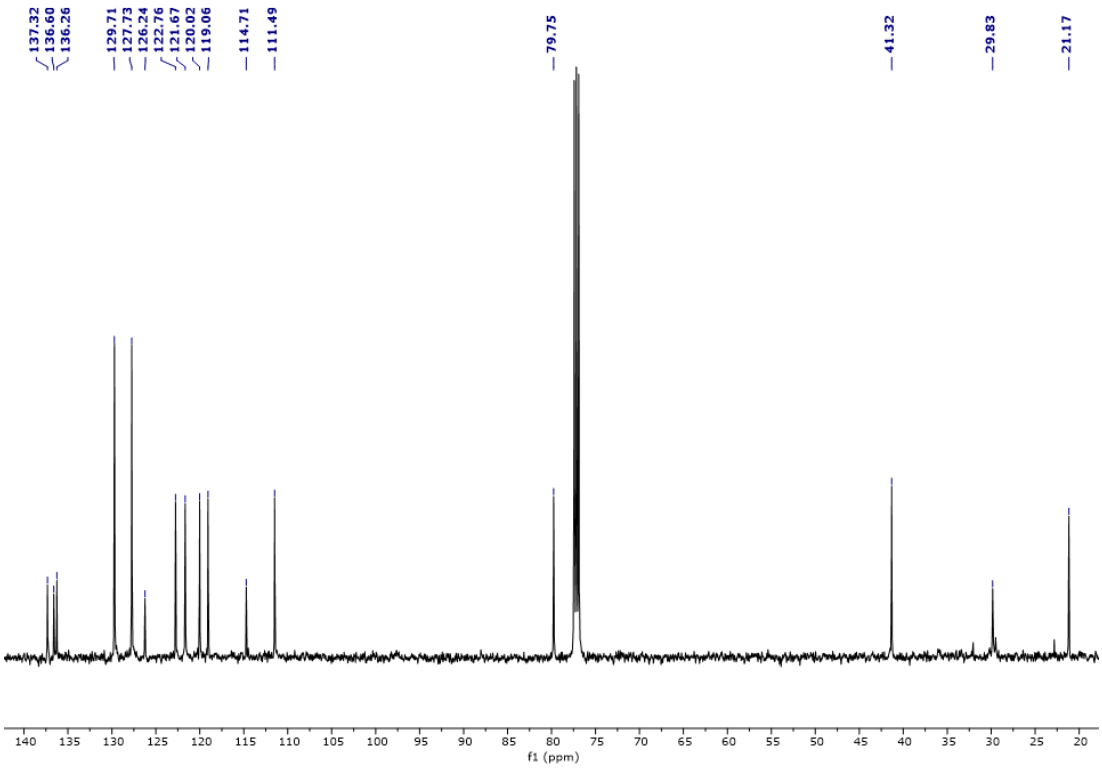

Figure S37. (a)^{1}H and (b) ^{13}C NMR spectra (Table 2, entry 3) of substrate scope 3-(2-nitro-1-(*p*-tolyl)ethyl)-1H-indole .

(a)

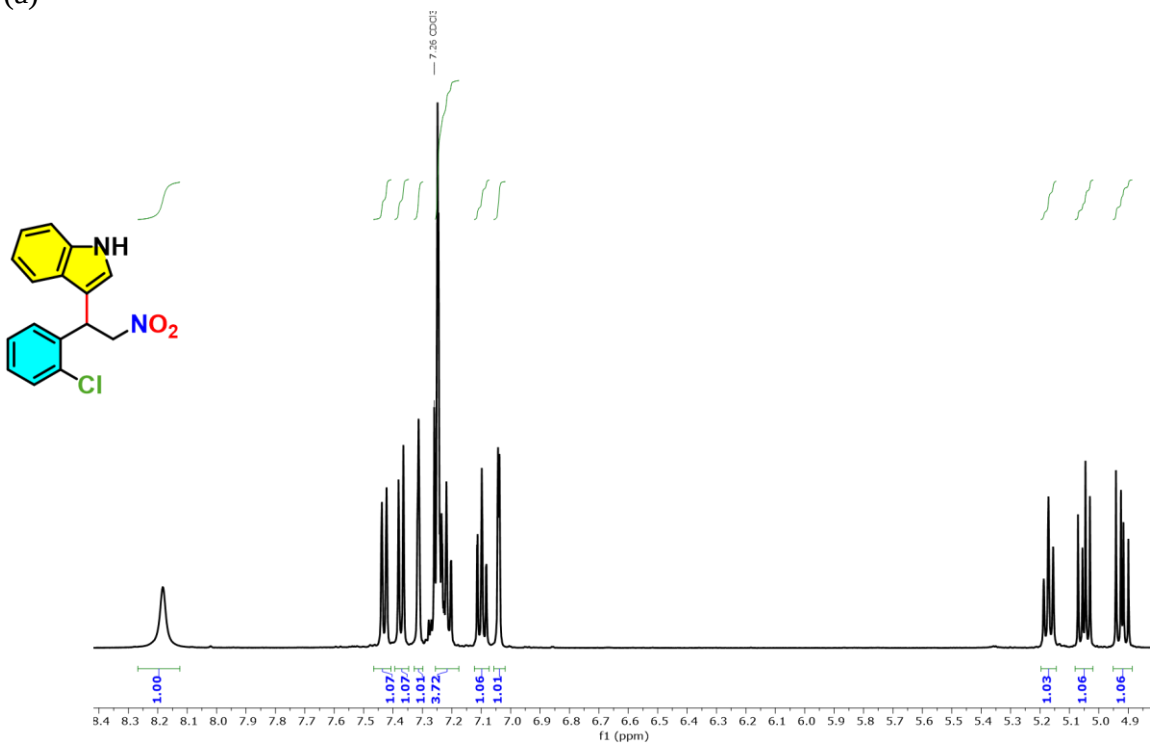

(b)

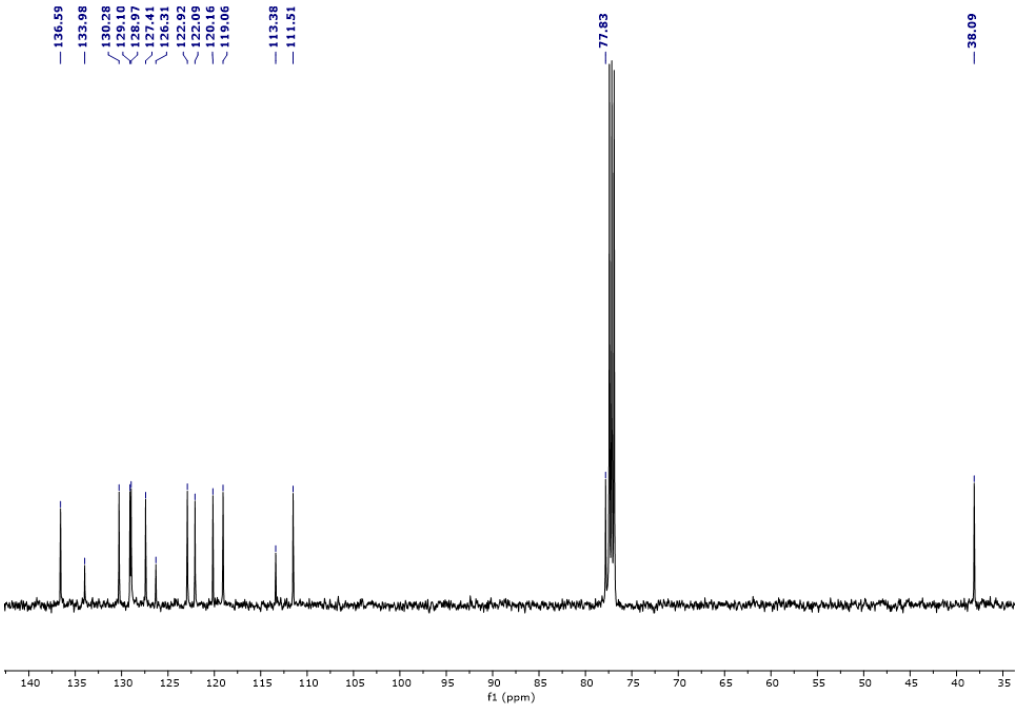

Figure S38. (a)^{1}H and (b) ^{13}C NMR spectra (Table 2, entry 4) of substrate scope 3-(1-(2-chlorophenyl)-2-nitroethyl)-1H-indole.

(a)

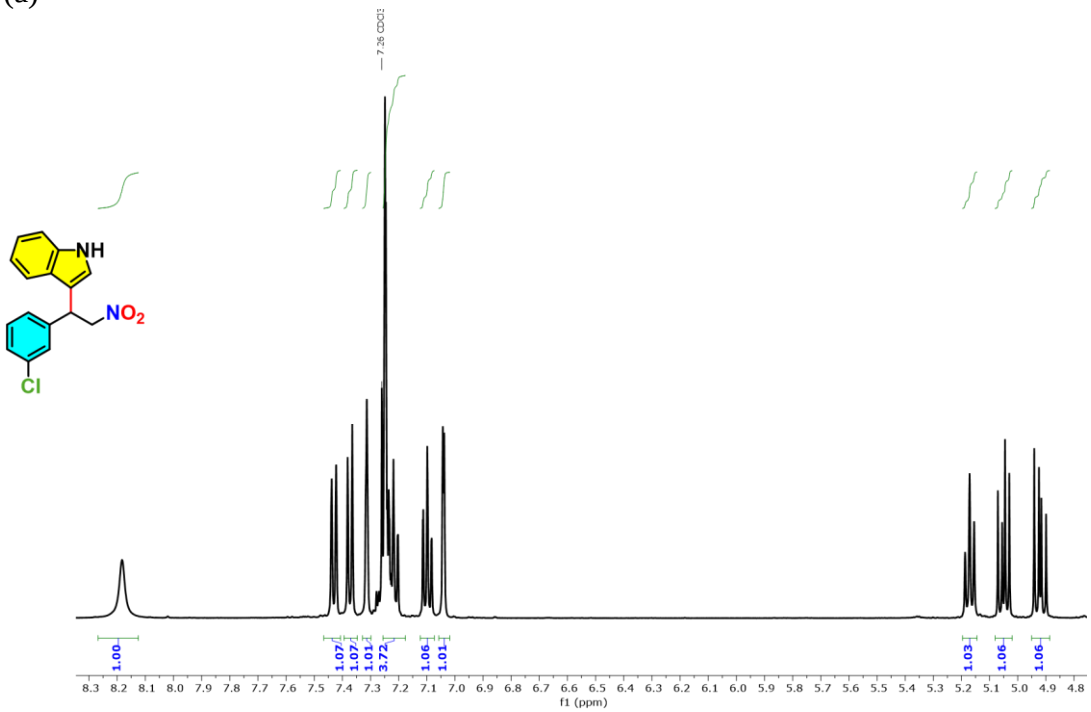

(b)

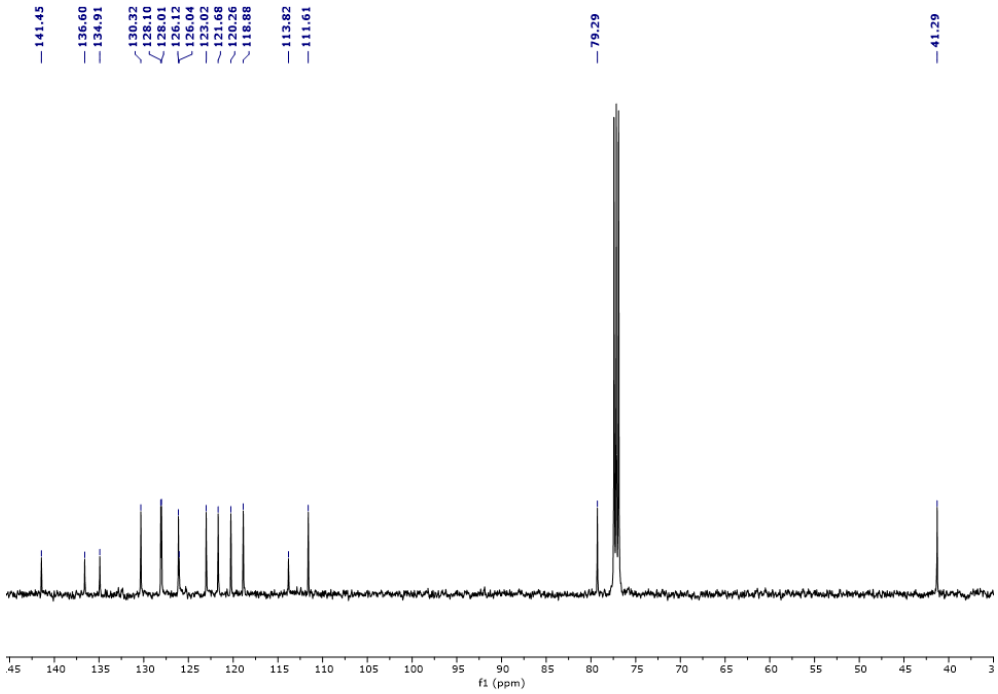

Figure S39. (a)^{1}H and (b) ^{13}C NMR spectra (Table 2, entry 5) of substrate scope 3-(1-(3-chlorophenyl)-2-nitroethyl)-1H-indole.

(a)

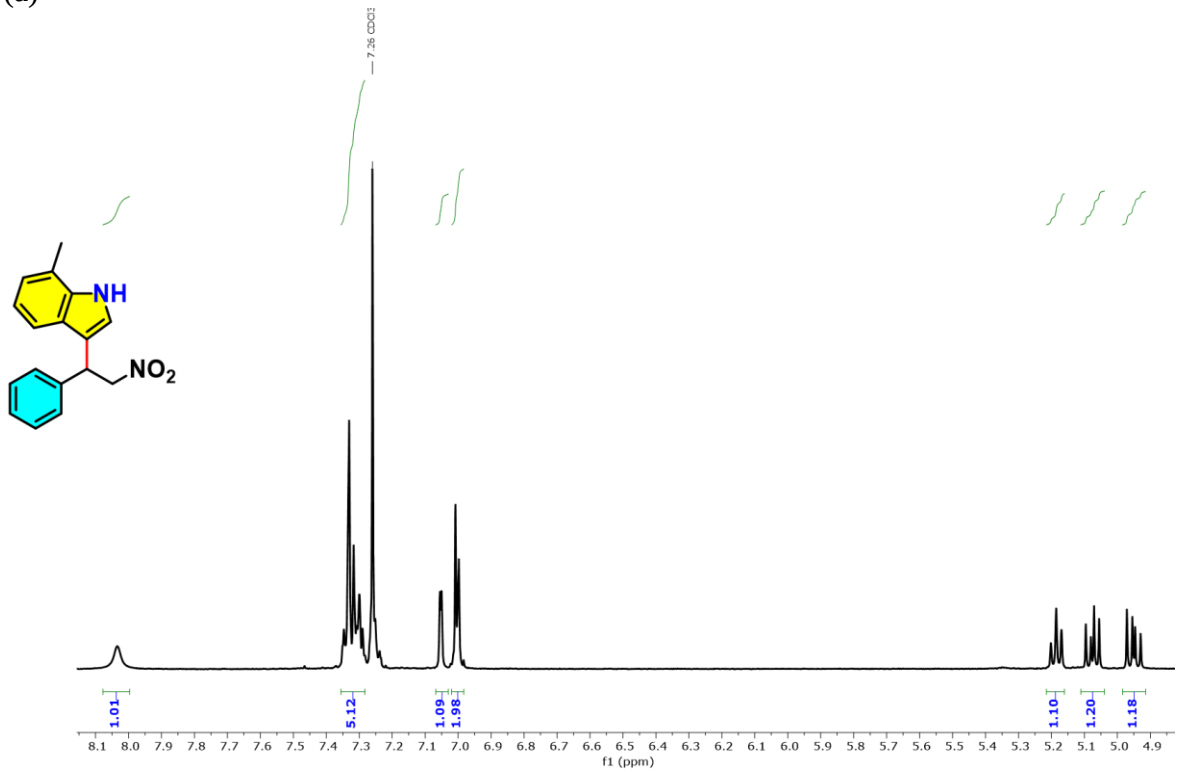

(b)

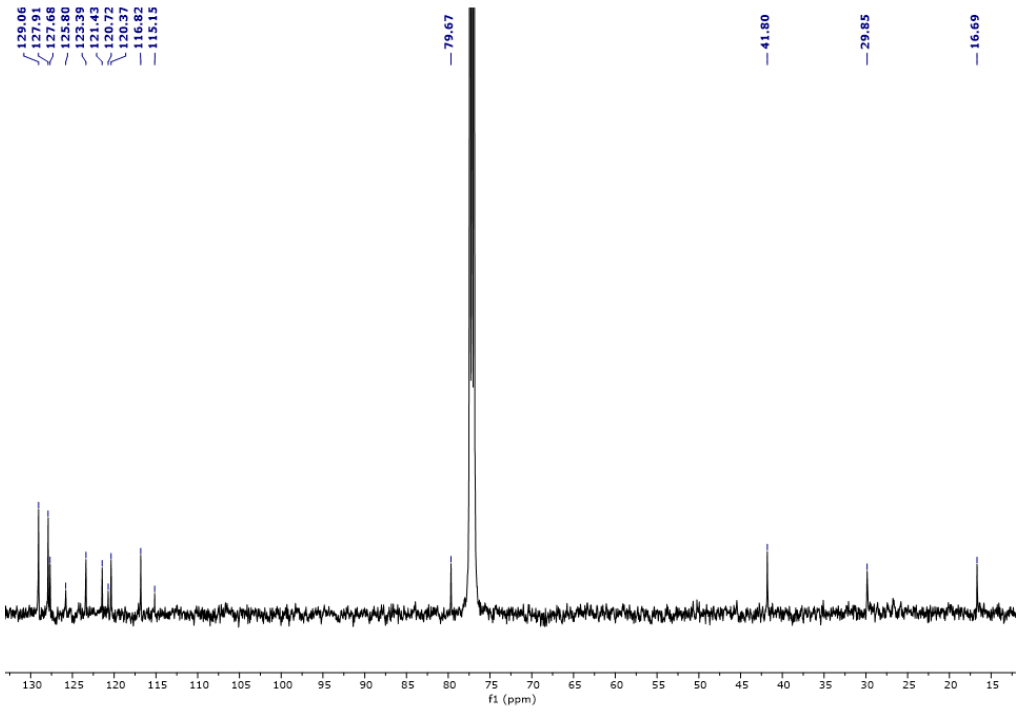

Figure S40. (a)^{1}H and (b) ^{13}C NMR spectra (Table 2, entry 6) of substrate scope 7-methyl-3-(2-nitro-1-phenylethyl)-1H-indole.

(a)

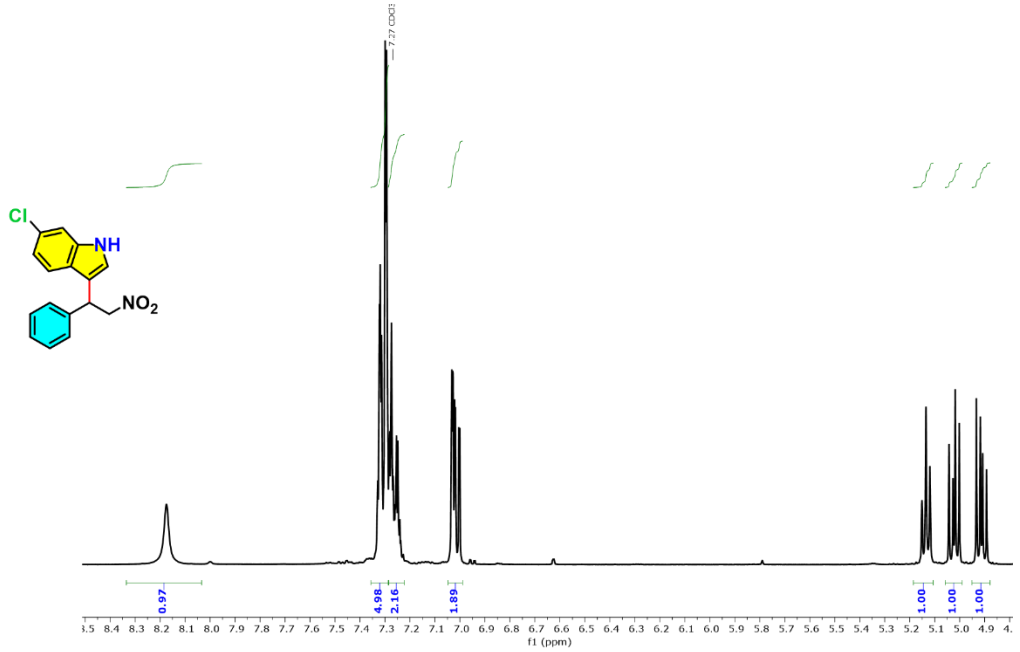

(b)

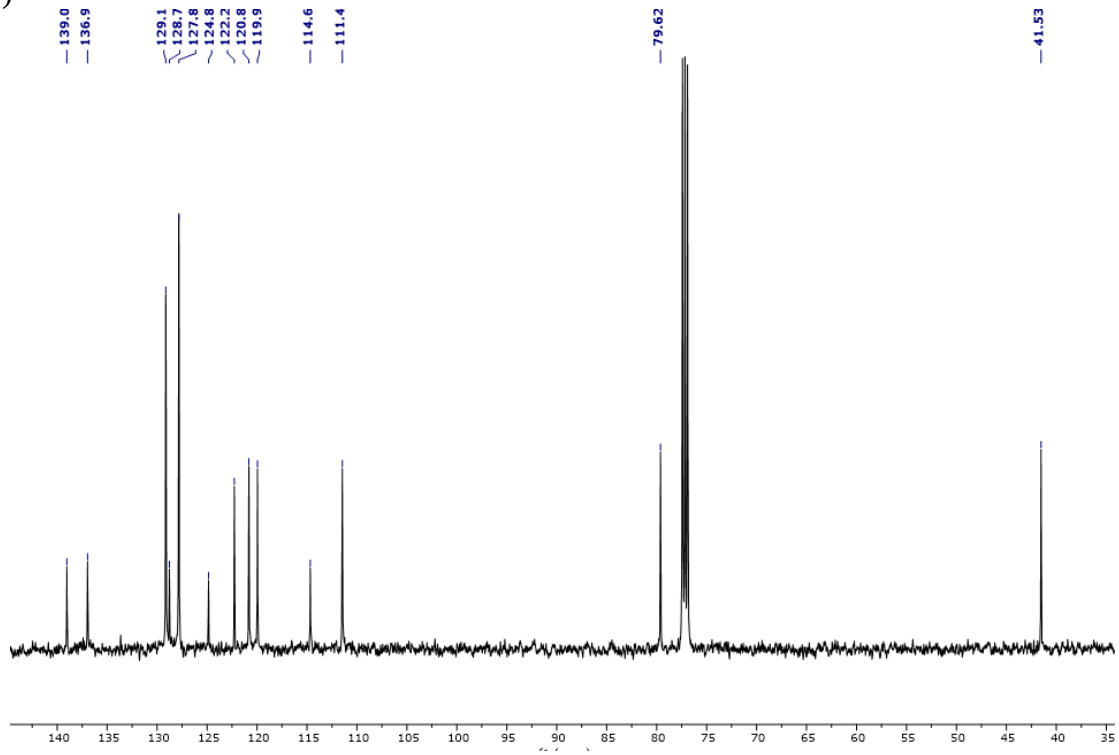

Figure S41. (a)^{1}H and (b) ^{13}C NMR spectra (Table 2, entry 7) of substrate scope 6-chloro-3-(2-nitro-1-phenylethyl)-1H-indole.

(a)

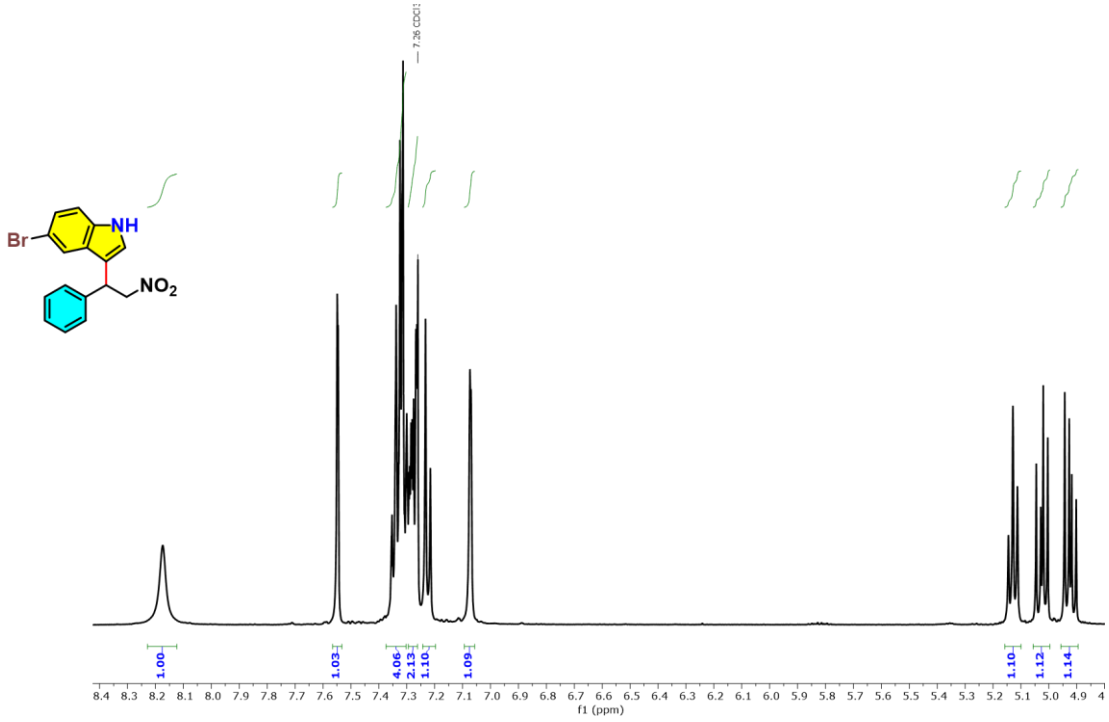

(b)

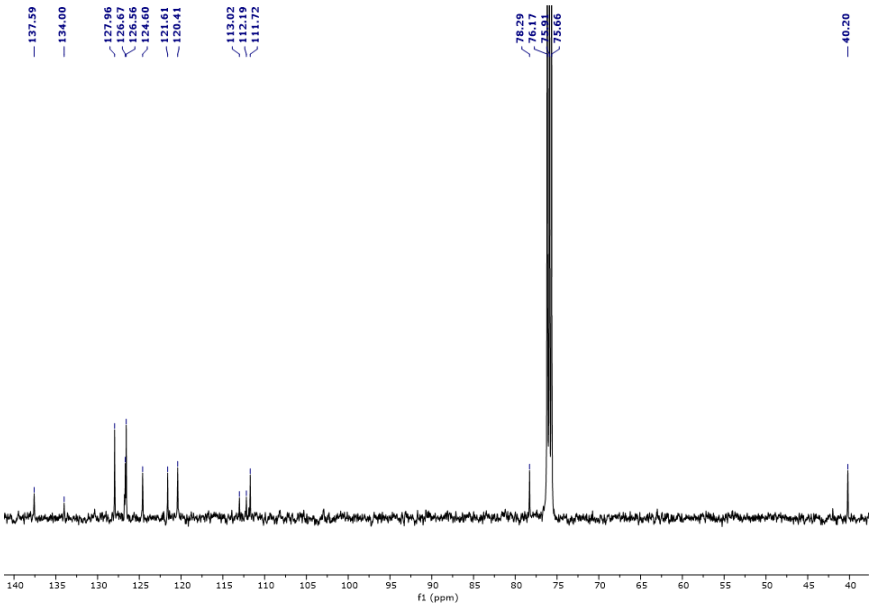

Figure S42. (a)^{1}H and (b) ^{13}C NMR spectra (Table 2, entry 8) of substrate scope 5-bromo-3-(2-nitro-1-phenylethyl)-1H-indole.

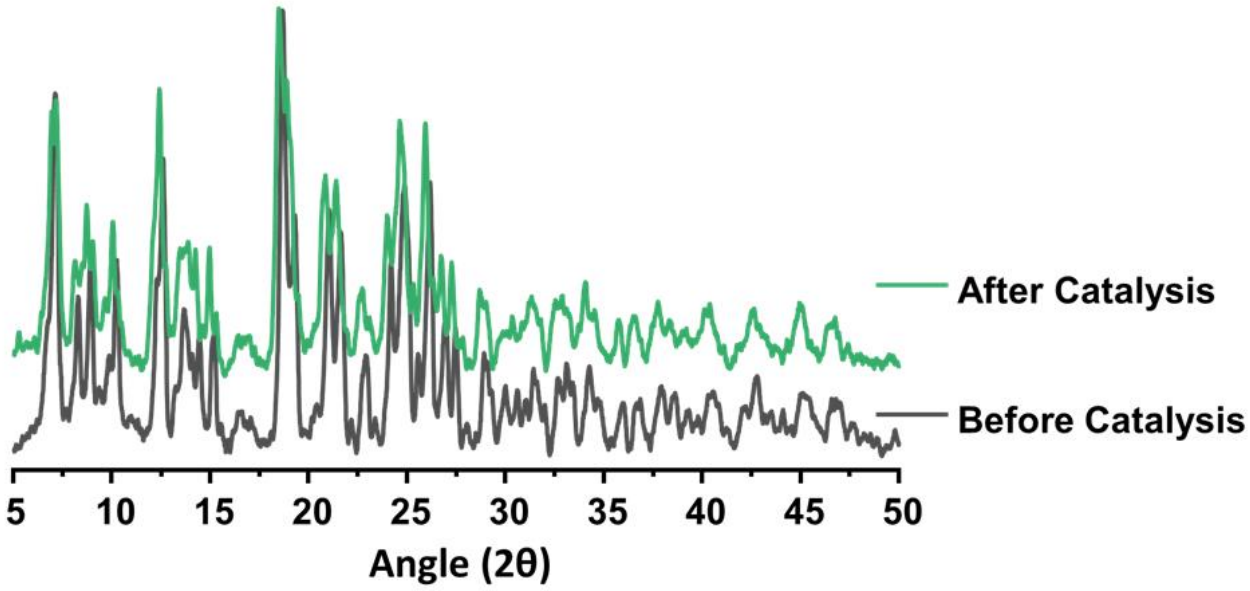

Figure S43. PXRD pattern of the catalyst before and after HBD reaction.

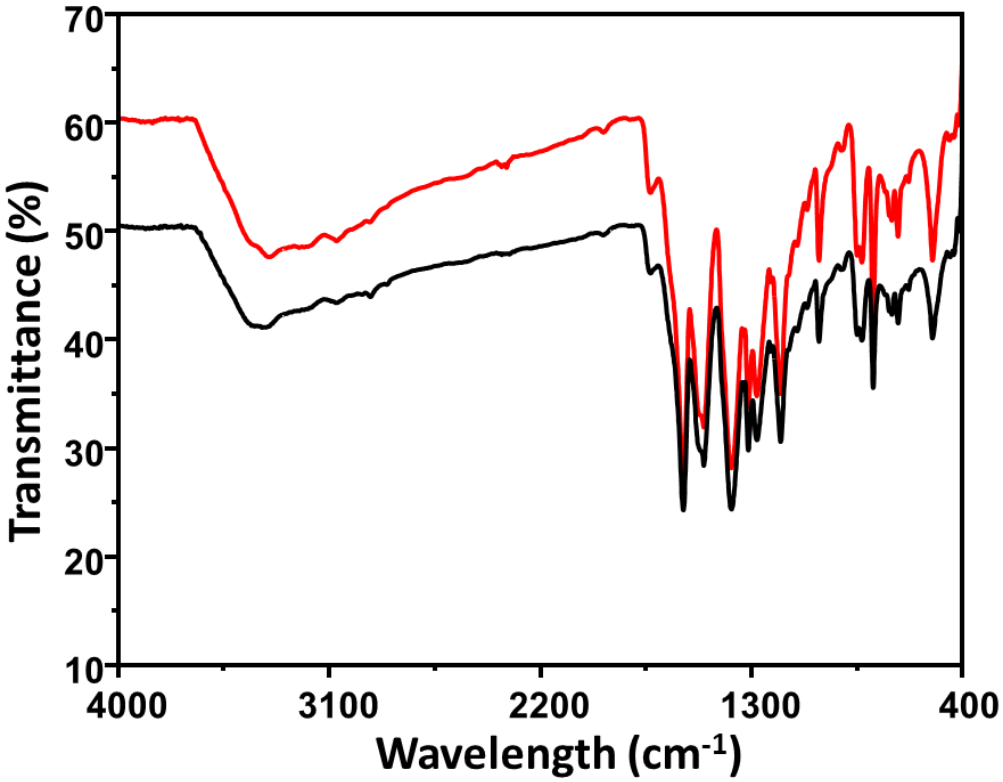

Figure S44. FTIR spectra of **12a** before and after catalysis.

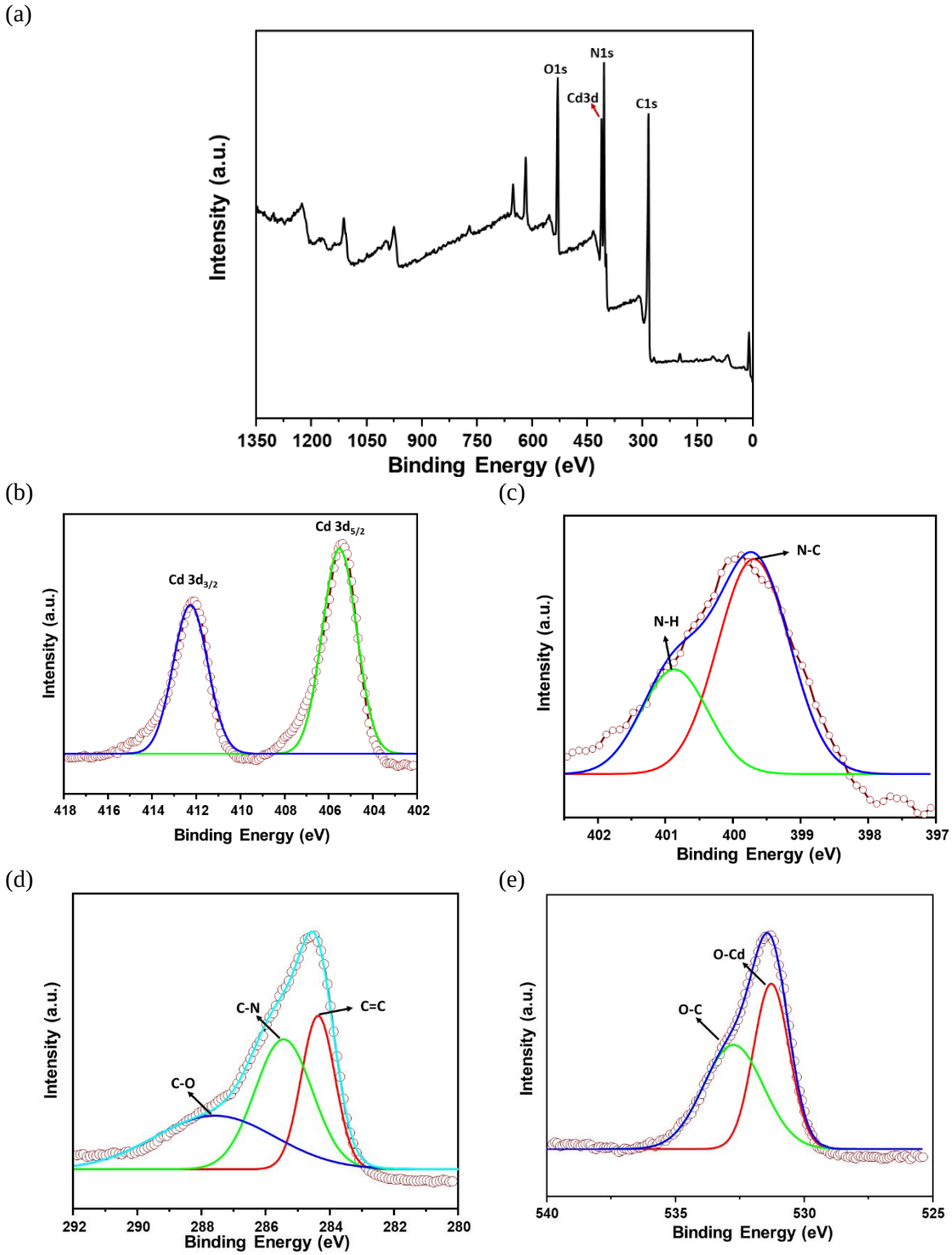

Figure S45. XPS spectra of **12a** after catalysis (a) survey spectra, deconvoluted spectra of (b) Cd 3d, (c) N 1s, (d) C 1s, and (e) O 1s.

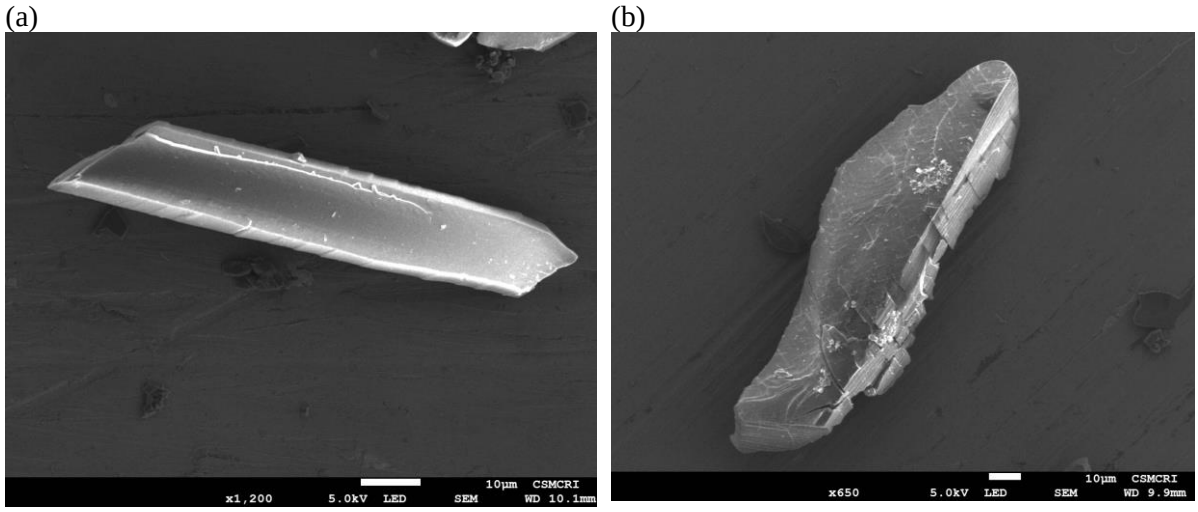

Figure S46. SEM images of **12a** (a) before and (b) after catalysis.

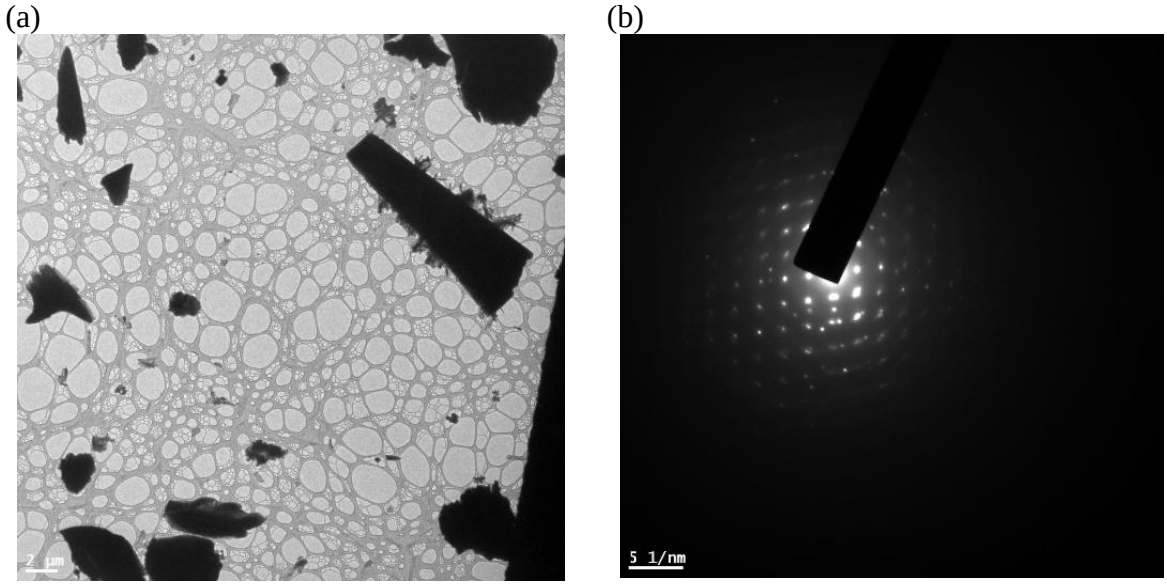

Figure S47. (a) TEM images and (b) SAED pattern for **12a** after catalysis.

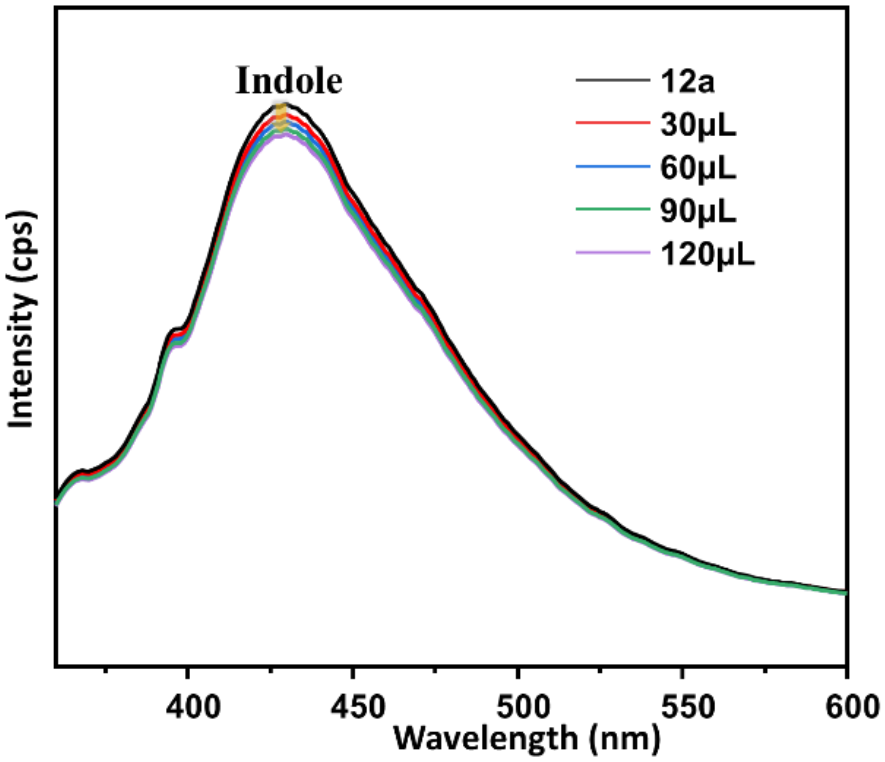

Figure S48. Change in the intensity of luminescence spectra of **12a** on addition of indole ($\lambda_{excitation}$: 360nm, slit width 2 nm)

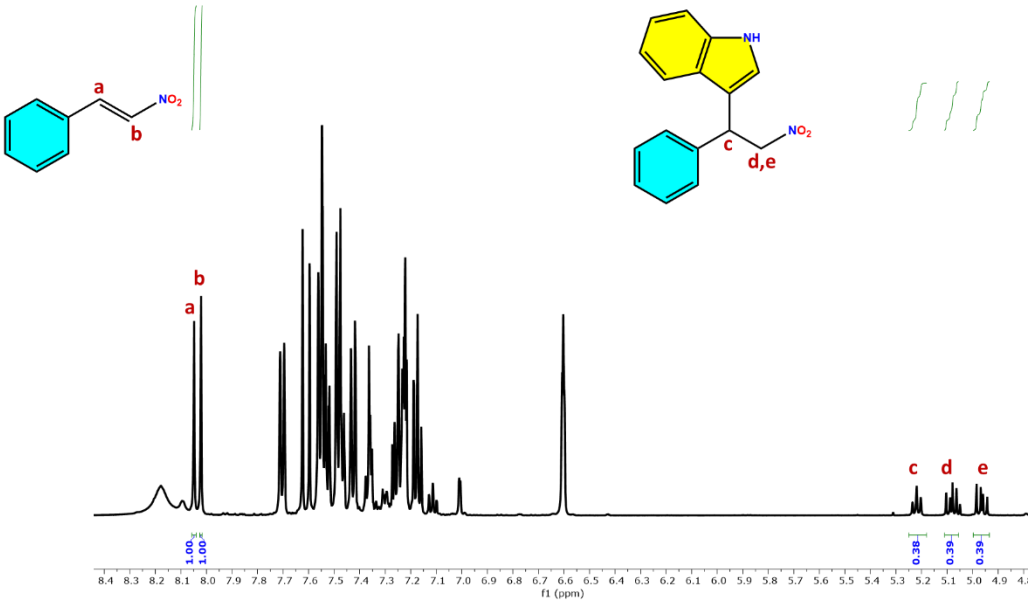

Figure S49. Integration in the ^{1}H NMR spectrum for the determination of conversion (%) of the reaction product catalysed by recovered catalyst without activation.

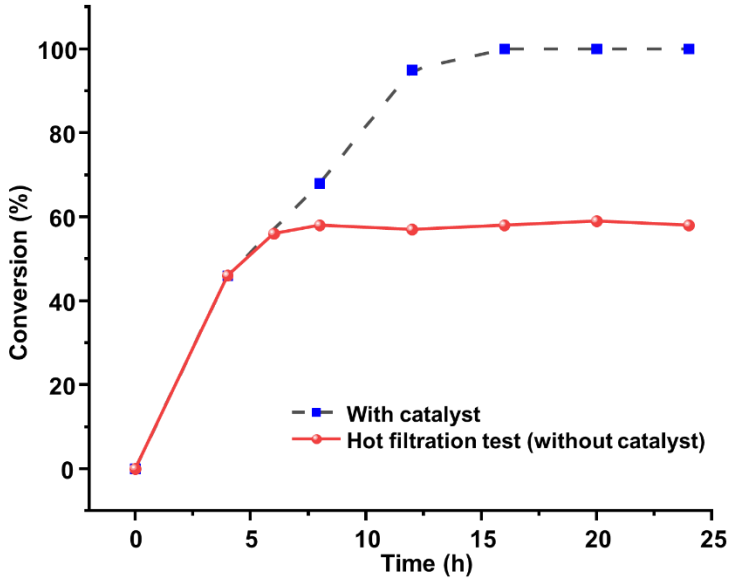

Figure S50. Time-conversion plot in the presence of **12a** (blue, dashed lines) and hot filtration test (red, solid line) upon filtration of catalyst after 6 h from the reaction mixture, and the reaction mixture maintained under identical conditions for the remaining time in the absence of catalyst.

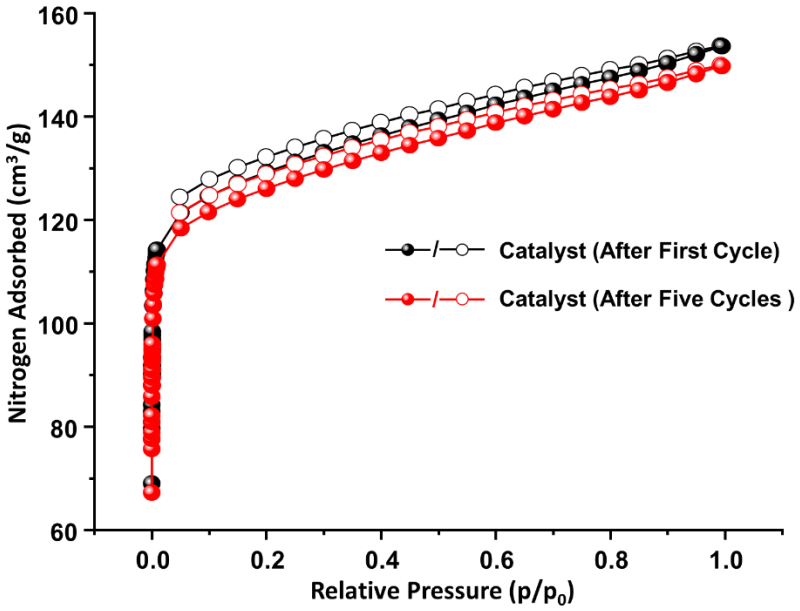

Figure S51. N_2 adsorption isotherm of **12a** after first cycle and five catalysis cycles.

Table S1. Crystal data and refinement parameters for **CSMCRI-12** and Product.

Identification code	**CSMCRI-12**	Product
Empirical formula	$C_{53}H_{36}Cd_3N_6O_{14}$	$C_{17}H_{16}N_2O_3$
Formula weight	1318.14	296.33
Temperature/K	180.15	150.15
Crystal system	triclinic	monoclinic
Space group	P-1	$P2_1/n$
a/Å	14.7456(3)	8.4800(7)
b/Å	14.8727(3)	9.5155(8)
c/Å	19.8711(5)	18.3484(17)
α/°	95.8630(10)	90
β/°	103.1660(10)	100.668(3)
γ/°	112.2630(10)	90
Volume/Å^3	3840.17(15)	1455.0(2)
Z	2	4
ρ_{calc}g/cm^3	1.1399	1.3527
μ/mm^{-1}	0.872	0.094
F(000)	1299.8	624.3
Radiation	Mo Kα (λ = 0.71073)	Mo Kα (λ = 0.71073)
2Θ range for data collection/°	4.72 to 52.82	4.84 to 56.66
Index ranges	$-18 \le h \le 18$, $-18 \le k \le 18$, $-24 \le l \le 24$	$-11 \le h \le 11$, $-12 \le k \le 12$, $-24 \le l \le 24$
Reflections collected	144882	27017
Independent reflections	15381 [R_{int} = 0.0700, R_{sigma} = 0.0389]	3604 [R_{int} = 0.0658, R_{sigma} = 0.0335]
Data/restraints/parameters	15381/0/687	3604/0/204
Goodness-of-fit on F^2	1.016	1.032
Final R indexes [I>=2σ (I)]	R_1 = 0.0535, wR_2 = 0.1474	R_1 = 0.0445, wR_2 = 0.1135
Final R indexes [all data]	R_1 = 0.0684, wR_2 = 0.1567	R_1 = 0.0552, wR_2 = 0.1194
Largest diff. peak/hole / e Å^{-3}	2.19/-1.45	0.40/-0.25
CCDC	2125430	2125432

Alert level B for Datablock: CSMCRI12

```
PLAT420_ALERT_2_B D-H Bond Without Acceptor O01A --H01A . Please Check
PLAT420_ALERT_2_B D-H Bond Without Acceptor O01A --H01B . Please Check
PLAT910_ALERT_3_B Missing # of FCF Reflection(s) Below Theta(Min). 12 Note
```

Explanation: All these alerts are generated because of some degree of disorder in the structure.

Determination of formula & solvent composition of CSMCRI-12 from PLATON Squeeze and Thermogravimetric analysis data:

From the TGA plot of as-synthesized **CSMCRI-12**, the observed mass loss is 21.27 % (initial 11.93 % + final 9.34 %).

From PLATON Squeeze program, void electron count / unit cell turns out to be 206.

As the asymmetric unit is electrically neutral and, DMA and water were used as solvents during the synthesis; so, the void space should be occupied by these lattice solvent molecules.

Now, formula of the asymmetric unit excluding all lattice guests is $[Cd_3(TCA)_2\boldsymbol{L}(H_2O)]$, with corresponding mass: 1316.13.

Table S2. Number of electrons and molecular mass of guest molecules, associated with **CSMCRI-12** for determination of solvent composition and molecular formula.

	Dimethyl acetamide (DMA)	Water
No. of electrons count	48	10
mass	82	18

Considering the above-mentioned number of electrons, the best possible combination of solvent molecules for **CSMCRI-12** could be $[Cd_3(TCA)_2\boldsymbol{L}(H_2O)]\cdot 2DMA\cdot 10H_2O$

The total number of electrons contributed by lattice solvent molecules will be [2×(48) + (10×11)] = 206, which is in agreement with the PLATON result and thus validates the above formula.

The aforementioned combination was further cross-checked from TGA analysis.

Total mass loss due to solvents is [2× (82) + (11×18)] = 362

Therefore, total mass of **CSMCRI-12** including all the guests is (1316.13+362) = 1678.13

So mass loss due to solvents is [(362/1678.13) ×100] % = 21.57 %, which is also comparable to that of the TGA result.

Table S3. List of metal-organic frameworks and their corresponding surface area.

S.No.	Chemical formula	Common name	BET (m^2/g)	Ref.
1.	$[Cu(bpy)_2(EDS)]_n$	TMOF-1	256	*Chem. Mater.*, **2016**, 28, 6276−6281
2.	-	UiO-66(Zr)-$(SH)_2$	308	*Angew. Chem., Int., Ed.*, **2015**, 54, 5142–5146
3.		NKMOF-1-Ni	382	*Angew. Chem. Int. Ed.*, 2018, **57**, 10971-10975
4.	$[Zn(hfipbb)(bpt)]_n \cdot n(DMF)_2 \cdot n(H_2O)$ (1)		-	*Cryst. Growth Des.* **2018**, *18*, 7570−7578
5.	UiO-66(Zr)-$(OCH_2CH_3)_2$		405	*Inorg. Chem.*, **2015**, *54*, 4862−4868
	UiO-66(Zr)-$(F)_4$		833	
6.	UiO-66(Zr)-$(COOH)_4$		212	
	$[Cu_2PDAI(H_2O)]$	PCN-124	1372	*Chem. Commun., 2012,48, 9995-9997*
7.		NU-1000	2320	*J. Am. Chem. Soc.*, **2013**, *13545*, 16801-16804
8.	$[CuL_2(NO_3)_2 \cdot$o-xylene DMF$]_n$	1□NO_3^-		*Chem. Eur. J.*, **2015**, *21*, 7071–7076
9.	$\{[Zn_2(TPOM)(3,7\text{-}DBTDC)_2] \cdot 7H_2O \cdot DMA\}_n$ (1)	1	28.2	*ACS Appl. Mater. Interfaces*, **2020**, *12*, 11724−11736
10.	$\{[Cd_2(TPOM)(3,7\text{-}DBTDC)_2] \cdot 6H_2O \cdot 3DMF\}_n$ (2).	2	37.8	
11.	$\{[Zn(SDB)(3,3'\text{-}L)_{0.5}] \cdot xG\}_n$	IITKGP-13A	206	*Inorg. Chem.*, **2020**, *59, 10*, 7056–7066
12.	$\{[Zn_2(SDB)_2(4,4'\text{-}L)] \cdot xG\}_n$	IITKGP-13B	129	
		MOF-5	3200*	*Microporous Mesoporous Mater.*, **2008**, *116*, 727–731
13.	$\{[Cu\text{-}(MTABA)(H_2O)] \cdot 4H_2O \cdot 2EtOH \cdot DMF\}_n$	Cu-MOF(1)	349.2**	*ACS Appl. Mater. Interfaces*, **2020**, *12*, 37137−37146
14.	$\{[Zn(CHDC)(L)].H_2O\}_n$ (1)	--	7	*Chem. Eur.J.*, **2018**, *24*,15831 –15839
15.	$\{[Cd(CHDC)(L)].H_2O\}_n$ (2)		19	

16.	{[$Zn_5(dmtrz)_3(IPA)_3(OH)$]·DMF·H_2O}$_n$	MAC-4	796	*Dalton Trans.*, **2012**, *41*, 4007–4011
	{[$Zn_5(dmtrz)_3$(OH-IPA)$_3(OH)$]·DMF·$5H_2O$}n	MAC-4-OH	339	
	[Cu(BDC-NO_2)(DMF)]·*x*Solvents	CuBDC-NO_2-a	523	*Inorg. Chem.* **2020**, *59, 23*, 17143–17148
17.	{[Co(BDC)(L)·$2H_2O$]·xG}$_n$	CoMOF-2	6.8	*Inorg. Chem.* **2019**, *58*, 10084−10096
18.	[$Zn_2Ca(bdc)_3(H_2O)_2$]$_n$•x(solvent)		586	*Inorg. Chem. Commun.*, **2020**, *121*, 108202
19.	Ni-MOF-1		152	*Inorg. Chem. Commun.*, **2019**, *104*,78-82
20.	{[Zn_2(TPOM)(3,7- DBTDC)$_2$]·$7H_2O$·DMA}$_n$		**267***	*ACS Appl. Mater. Interfaces,* **2020,** *12*, 11724−11736
21.	{[Cd_2(TPOM)(3,7- DBTDC)$_2$]·$6H_2O$·3DMF}		**432***	
22.	[Cd(***L1***)$_2$] ·2DMF	CSMCRI-7	**19**	*J. Mater. Chem. C*, **2021**, *9*, 7142–7153
	[Cd(***L2***)$_2$] ·2DMF	CSMCRI-8	**23**	
	$(CH_3)_2NH_2$·[$Co_3(TCA)_2$(μ_2-OH)$(bpy)_{1.5}(H_2O)_3$]·1.5DMF·$1.5H_2O$	CSMCRI-10	**63**	*ACS Appl. Mater. Interfaces,* **2021, *13,*** 28378−28389
23.	[$Cu_{1.5}$(TCA)(bpy)]·DMF·$1.5H_2O$	CSMCRI-13	**79**	*ACS Appl. Mater. Interfaces,* **2021,** 13, 46, 55123–55135
24.	[$Cd_3(TCA)_2$(***L***) ·H_2O]·2DMA·$11H_2O$	**CSMCRI-12**	**503**	***This Work***

*From CO_2@195K

Table S4. Comparison of Various HBD Catalysts in the Friedel−Crafts Alkylation Reaction of Indole and β-nitrostyrene.

Entry	Catalyst	mol (%)	time (h)	solvent	temp (°C)	yield (%)	Ref.
1	UiO-67-Squar/bpdc	10	24	Toluene-d_8	50	95	***J. Am. Chem. Soc.* 2015, *137*, 919−925**
2	UiO-67-Squar/bpdc	10	24	Dichloromethane	RT	78	***J. Am. Chem. Soc.* 2015, *137*, 919−925**
3	$Cu_4(dbda)_2 \cdot (CH_3OH)_4$	5	24	Chloroform	50	>99	***Chem. Commun.* 2016, *52*, 8585−8588**
4	Cr-MIL-101-UR3	15	24	Acetonitrile	60	93	***Chem. Commun.* 2013, *49*, 7681−7683**
5	$[Zn_4O(L1)(DMF)_2] \cdot 3DMF$	22	24	Toluene	60	90	***ChemCatChem* 2017, *9*, 1172−1176**
6	$[CuL2 \cdot H_2O] \cdot 2DMF \cdot H_2O$	1.5	18	Acetonitrile	60	98	***Catal. Commun.* 2018, *104*, 123−127**
7	$\{[Zn_2(2\text{-}BQBG)(BDC)_2] \cdot 10H_2O\}_n$	3	12	CH_2Cl_2	35	100	**ACS Catal. 2019, 9, 3165−3173**
8	NU-GRH-1 + TMS-Cl (18 mol %)	3	4	Toluene-d_8	60	98	***ACS Catal.* 2016, *6*, 3248−3252**
9.	$[Zr_6O_4(OH)_4(L)_6] \cdot 7H_2O \cdot 3DMF$	10mg*	24	toluene	70	97	***Inorg. Chem.* 2019, 58, 5163-5172**
10.	**CSMCRI-12**	**10**	16	Toluene	**60**	**96**	**This work**

[a] H_4dbda = 5,5′-(3,4-dioxocylcobut-1-ene-1,2-diyl)*bis*(azanediyl)diisophthalic acid, L1 = 4,4′-ureylene-benzene dicarboxylate L2 = 5-(3-phenylureido)-benzene-1,3-di(4-phenylcarbo xylate), BQBG = 2,2′-(butane-1,4-diylbis-((quinolin-2-ylmethyl)azanediyl))diacetamide

Reference

(1) Hanwell, M. D.; Curtis, D. E.; Lonie, D. C.; Vandermeersch, T.; Zurek, E.; Hutchison, G. R. Avogadro: An Advanced Semantic Chemical Editor, Visualization, and Analysis Platform. *J. Cheminf.* **2012**, *4*, 17, DOI: 10.1186/1758-2946-4-17
(2) APEX2, v. 2014.7-1; Bruker AXS: Madison, WI, 2014.
(3) SAINT, v. 8.34A; Bruker AXS: Madison, WI, 2013.
(4) SADABS, v. 2014/3; Bruker AXS: Madison, WI, 2013.
(5) Dolomanov, O. V.; Bourhis, L. J.; Gildea, R. J.; Howard, J. A. K.; Puschmann, H. *J. Appl. Crystallogr.* **2009**, *42*, 339−341.
(6) Sheldrick, G. M. SHELXTL Version 2014/7. https://shelx.uniac.gwdg.de/SHELX/index.php.
(7) Spek, A. L. PLATON; The University of Utrecht: Utrecht, The Netherlands, 1999.
(8) http://www.topos.ssu.samara.ru; Blatov, V. A. IUCrCompCommNewsletter 2006, 7, 4
(9) Seal, N.; Goswami, R.; Singh, M.; Pillai, R. S.; Neogi, S., An Ultralight Charged MOF as Fluoro-Switchable Monitor for Assorted Organo-Toxins: Size-Exclusive Dye Scrubbing and Anticounterfeiting Applications via Tb^{3+} Sensitization. *Inorg. Chem. Front.* **2021**, *8*, 296-310.